IMPACT OF LAND USE LAND COVER CHANGE ON HYDROLOGIC RESPONSE: THE CASE OF DEME CATCHMENT, OMO-GIBE RIVER BASIN, ETHIOPIA

MASTERS OF SCIENCE THESIS

MULUKEN ISRAEL BIRRU

HAWASSA UNIVERSITY, HAWASSA, ETHIOPIA

DATE OF SUBMISSION: February 24, 2021

IMPACT OF LAND USE LAND COVER CHANGE ON HYDROLOGIC RESPONSE: THE CASE OF DEME CATCHMENT, OMO-GIBE RIVER BASIN, ETHIOPIA

MULUKEN ISRAEL BIRRU

A THESIS SUBMITTED TO THE
FACULTY OF BIO-SYSTEMS AND WATER RESOURCE ENGINEERING
DEPARTMENT OF WATER RESOURCE AND IRRIGATION ENGINEERING
HAWASSA UNIVERSITY INSTITUTE OF TECHNOLOGY
SCHOOL OF GRADUATE STUDIES
HAWASSA UNIVERSITY
HAWASSA, ETHIOPIA

IN PARTIAL FULFILLMENT OF THE
REQUIREMENTS FOR THE
DEGREE OF

MASTERS OF SCIENCE IN WATER RESOURCE AND IRRIGATION ENGINEERING
(SPECIALIZATION: WATER RESOURCE ENGINEERING AND MANAGEMENT)

SCHOOL OF GRADUATE STUDIES

HAWASSA UNIVERSITY

EXAMINERS APPROVAL SHEET-2

We, the undersigned, members of the Board of Examiners of the final open defense by Muluken Israel Birru have read and evaluate his/her thesis entitled "Impact of Land Use Land Cover Change On Hydrologic Response: The Case of Deme Catchment, Omo-Gibe River Basin, Ethiopia", and examined the candidate. This is, therefore, to certify that the thesis has been accepted in partial fulfillment of the requirements for the degree of master's science.

_____	_____	_____
Name of Major Advisor	Signature	Date
_____	_____	_____
Name of Internal Examiner-I	Signature	Date
_____	_____	_____
Name of Internal Examiner-II	Signature	Date
Tekalegn Ayele Woldesenbet (PhD)	_____	19/04/2021
Name of External Examiner	Signature	Date
_____	_____	_____
SGS Approval	Signature	Date

Final approval and acceptance of the thesis is contingent upon the submission of the final copy of the thesis to the School of Graduate Studies (SGS) through the Department/School Graduate Committee(DGC/SGC) of the candidate's department.

Stamp of SGSDate

Remark

(Use this form to submit the thesis with minor correction suggested by the examining board).

SCHOOL OF GRADUATE STUDIES

HAWASSA UNIVERSITY

ADVISORS APPROVAL SHEET

This is to certify that the thesis entitled "IMPACT OF LULCC ON HYDROLOGIC RESPONSE: THE CASE OF DEME CATCHMENT, OMO-GIBE RIVER BASIN, ETHIOPIA" submitted in partial fulfillment of the requirements for the degree of masters with specialization in water resource engineering and management, Department of the water resource and irrigation engineering, and has been carried out by MULUKEN ISRAEL ID NO. PGWREMR/0012/11, under our supervision. Therefore, we recommend that the student has fulfilled the requirements and hence hereby can submit the thesis to the department.

Major Advisor: Dr. Nigatu Wondrade _____ _____

Signature Date

Co-Advisor: Sisu Biru _____ _____

Signature Date

ACKNOWLEDGEMENT

Above all and for the most, my praise and thanks go to the almighty God who enables me to perform things through his strengthening arm and guides me to the complete success that has been predestined by him. My deepest heartfelt gratitude and appreciation is for my Major Advisor Dr. Nigatu Wondrade and Co-Advisor Sisu Biru for their invaluable guidance and consultation through my research studies by spending most of their time to give me advice.

I extend my appreciation to all organizations and individuals who helped me in my study. First I would like to thank Dilla university for its financial support. The last but not least, I would like to acknowledge the Ministry of Water, irrigation and Electricity of Ethiopia, and the Ethiopian Meteorological Agency for giving me the necessary data. Finally, I appreciate my family who supported and strengthened me morally.

DECLARATION

I hereby declare that this MSc thesis is my original work and has not been presented for a degree in any other university, and all sources of material used for this thesis have been duly acknowledged.

Name Muluken Israel

Signature: _____

This MSc thesis has been submitted for examination with my approval as Thesis advisor.

Name: Nigatu Wondrade

Signature: _____-

Place and date of submission:

Place and date of submission: Hawassa University, February 24, 2021

LIST OF ABBREVIATIONS AND ACRONYMS

asl	Above Sea Level
DEM	Digital Elevation Model
SCS	Soil Conservation Service
AOI	Area of Training
DMC	Double Mass Curve
FAO	Food and Agricultural Organization/
UNESCO	United Nation Education, Scientific and Cultural Organization
GC	Gregorian Calendar
GIS	Geographic Information System
GWQ	Ground Water Flow
HBV	Hydrologisika BayraansVttenbalans-avediling
HEC-HMS	Hydraulic Engineering Centre-Hydrologic Modeling System
HRU	Hydraulic Response Unit
LATQ	Lateral Flow
LULCC	Land Use Land Cover Change
MoWIE	Ministry of Water, Irrigation, and Energy
MRS	Mean Relative Sensitivity
MSS	Multi-Spectral Scanner
NMSA	National Meteorological Service Agency
NSE	Nash-Sutcliffe Model Efficiency
PBIAS	Percent Bias
PET	Potential Evapotranspiration
R2	Coefficient of Determination
RGB	Red Green Blue
SSE	Supervised Spatial Encoder
SUFI2	Sequential Uncertainty Fitting
SURQ	Surface Run-Off
SWAT	Soil and Water Assessment Tool
SWAT-CUP	SWAT Calibration and Uncertainty Program
TM	Thematic Mapper
UTM	Universal Traverse Mercator
WEGEN	Weather Generator
WGEN	Weather Generator

TABLE OF CONTENTS

LIST OF TABLES

LIST OF FIGURES

LIST OF APPENDICES

ABSTRACT

Hydrologic modeling was conducted for each LULC map in three time periods (1999, 2010, 2018) in the Deme catchment using the SWAT model. Changes in streamflow and its components between three simulations by using the LULC map of 1999, 2010, and 2018 were related to the changes of LULC to quantify the impact of LULCC. The data used for analyses were streamflow of Deme catchment, satellite imageries of 1999,2010, and 2018, Digital elevation model, and meteorological data. LULC classification was carried out by using ERDAS imagine2014. Five types of LULC were identified in the Deme watersheds such as agricultural land, grassland, bushland, built-up area, and forest. The LULCC analysis depicted that there was an expansion of agricultural land and the built-up area in the catchment. Agricultural land was increased by 29.96% and 36.78% from 1999-2010 and 2010 -2018 respectively. The built-up area was also increased by 80.41% and 148.47% during the first and the second period respectively. The other LULC classes showed a continuous decrement in all periods. The performance evaluation result depicted that the SWAT model can be used for the analysis of the impact of LULCC on streamflow of the Deme catchment. During calibration, the value for NSE, $R^{2,}$ and PBIAS was 0.80, 0.75, and -1.2 respectively. During validation, the value for NSE, $R^{2,}$ and PBIAS was 0.74, 0.70, and -7.3 respectively. The LULCC had impacted the magnitude of streamflow and its components. During the driest season, mean monthly streamflow has decreased by 16.71% and 37.81% during the first and second periods respectively. But in contrast during the wettest month, the mean monthly streamflow has increased by 12.79% and 25.16% during the first and second period respectively. The contribution of mean annual surface runoff increased by 11.63mm and 15.94mm from 1999-2010 and 2010 to 2018 respectively. While lateral flow decreased by 6.47mm and 9.96mm in both periods. Similarly, shallow groundwater recharge decreased by 3.77mm and4.67mm during the first and second periods. The decrease in lateral flow and shallow groundwater recharge and increase in surface runoff was related to the expansion of agricultural land, and built-up area, as well as decrement of forest, bushland and grass land. Therefore, Deme watershed requires the application of appropriate watershed management options to minimize the undesirable impacts on water and land resources.

KEYWORDS: Deme watershed, SWAT model, LULCC, Streamflow.

1. INTRODUCTION

1.1.Background

Throughout human history, the land has been tightly attached to economic, social, infrastructures, and other human activities (Lambin et al., 2003). For centuries humans have been altering the earth's surface to produce food through agricultural activities (Assefa 2012). In the past few decades' conversion of grassland, woodland, and forest into agricultural land and pasture land has risen dramatically, especially in developing countries where a large proportion of the human population depends on natural resources for their livelihoods (FAO 2005). The increasing demand for land often results in changes in LULC (Assefa, 2012). LULCC is a widespread, accelerating, and significant process driven by human actions (Leh et al., 2011). Factors driving LULCC include an increase in population number and population response to economic opportunities (Lambin et al., 2001). Population pressure is a major driving force in LULCC (Woldamlak, 2002). For instance, between 1990 and 2015, East Africa forest cover decreased annually by about 1% while the human population increased an average annual rate of 2% (Guzha et al., 2018).

On top of the rapid change in LULC of forest land, grazing land or bush lands to cultivated lands is becoming a common practice in most parts of Ethiopia (Amanuel and Mulugeta, 2014). Rain-fed agriculture is the major economic activity of the country employing over 85% of the population (Devereux, 200). Ethiopia's forest has suffered severe deforestation and degradation from increased demand for fuel wood, construction wood, and cropping and grazing land (Wogayehu, 2003). South western Ethiopia is environmentally challenged mainly due to resource degradation, soil erosion, and nutrient depletions. One such form of resource degradation was believed to follow from LULCC (Wakjira et al., 2016).

LULCC have a potentially large impact on water resources (Stonestorm et al., 2009). The impact of LULCC on hydrology are especially important as they are related to the change and

availability of water resources that are essential for both human being and ecosystem (Oki and Kanae, 2006). Van der Ent et al. (2010) noted that globally 40% of the territorial precipitation originates from land evapotranspiration and that 57% of all terrestrial evapotranspiration returns as precipitation over land. LULCC directly affects streamflow, by changing the interception rate, root water uptake, and infiltration (Lan, 2016). LULCC is becoming the challenge that hinders the implementation of IWRM in the Omo-Gibe river basin (Yericho and Mulugeta, 2019). Deme catchment is part of the Omo-Gibe river basin. Additionally, some studies showed that the presence of LULCC. Milkias (2019), reported the expansion of urbanization in his study under the title urban land use conflict in the expansion area of Wolaita Sodo town. Nowadays quantifying the impact of LULCC on streamflow has been given more attention (Jiang et al., 2011; Yang et al., 2012).

1.2.Statement of the problem

In Ethiopia, the severity of LULC changes as a result of population increment, expansion of the agricultural sector, and development of Urban areas are happening at an alarming rate (Getachew and Melesse, 2012). Deme catchment is part of the middle west of the Omo gibe river basin, which is densely populated from other parts of the Omo-Gibe river basin (Yericho and Mulugeta, 2019). Based on the Data from Kucha woreda agricultural and development bureau (2014) the population density in the Deme catchment was 123.2 people/Km^2. This population pressure causes various effects on resource bases like deforestation, expansion of residential areas, and agricultural land. This activity leads to the condition of land under little vegetation cover.

The connection and interaction of water with LULC, natural ecosystem, and hydrology are complicated with a wide variety of spatial and temporal scales. The hydrologic cycle illustrates the many pathways by which water interacts with land or natural ecosystem. This pathway can be affected by several factors such as LULCC (Mustard and Fisher, 2004). LULCC has a great

influence on the hydrologic response of a watershed (Kirby et al., 2016). LULCC can lead to significant changes in leaf area index, evapotranspiration, soil moisture content, and infiltration capacity (Mao and Cherkuer, 2009). This significant change impacts surface and subsurface flow regimes including base flow contribution to streamflow (Tu, 2009). Streamflow, infiltration, surface runoff, and groundwater flow are the hydrologic components that could be affected by LULCC (Natkhin et al.,2015). The continuous LULCC can influence the water balance by changing the magnitude and patterns of components of streamflow such as surface runoff, lateral flow, and groundwater flow; which in turn increases the extent of the water management problem (Tekleab, 2015). The spatial and temporal variability of LULCC has a paramount impact on the presence of quantity and quality of river water flow (Tadele, 2009). The Deme catchment is facing problems related to the consequences of LULCC on streamflow. The streamflow magnitude of the Deme catchment was disturbed.

There are no studies conducted on the Deme catchment related to LULCC and its impact on streamflow. However, LULCC is becoming the challenge that hinders the implementation of IWRM in the Omo-Gibe river basin (Yericho and Mulugeta, 2019). Deme catchment is part of the Omo-Gibe river basin. Nowadays, hydrological models are used to represent the hydrological characteristics (Surur, 2010). Models are particularly useful, as they can assess past as well as possible future impact using LULC scenario. This study integrates the SWAT model and ERDAS imagine2014 to evaluate the impact of LULCC on the Deme catchment. The main intention was to quantify LULCC in the watershed and its impact on streamflow.

1.3.The objective of the study

1.3.1. General objective

The main objective of the study is to evaluate the impact of land use land cover change on the streamflow of the Deme catchment.

1.3.2. Specific objectives

To estimate land use land cover change dynamics of Deme catchment using multi-temporal satellite images (1999, 2010, and 2018).

- To estimate land use land cover change dynamics of Deme catchment using multi-temporal satellite images (1999, 2010, and 2018).
- To evaluate the effect of land use land cover change on the streamflow of Deme catchment for the past 30 years by using the Hydrologic model (SWAT).

1.4.Research question

- To what extent has the spatial and temporal land cover change in the Deme catchment occurred?
- How does the land use land cover change affect the annual flow of the Deme river?
- How will LULCC affect the seasonal flow of the Deme river?
- How will surface runoff and groundwater recharge respond to LULCC?

1.5.Scope of the study

This study is limited to the Deme catchment and only focuses on the impact of land use land cover change on the streamflow of the river. The study area covers upstream of the gauging station which is named Orata-alem. This station has been in operation since 1985, therefore the data (i.e. spatial data, meteorological data, and hydrologic data) is used in this study starts from 1987. The study is used 30m*30m DEM for watershed delineation. The SWAT model is used to analyze the impact of LULC change on the streamflow. The year for the selection of satellite images was based on historic events, previous studies, and the availability of images. Recorded streamflow data for the river was available from 1987 to 2006 only therefore the analysis was based on this available data.

1.6.Significance of the study

In Ethiopia where about 85% of the population is engaged in agriculture and depends on available water resources, the assessment and management of available water resources is a matter of prime importance (Bezawit, 2011). As water is a valuable part of our ecosystem that individuals have to be granted, predicting its availability for the next generation has become an essential task in planning and resource management for rapidly developing areas (Wakjira et al., 2016). Land use planning and management are closely related to the sustainability of water resources (Guo et al., 2008).

This necessitates, exploring and integrating the significance of LULCC on the hydrologic processes, such as changes in water demand and supply with emerging on land change science. The evaluation of LULCC on the hydrologic process is vital to predicting reasonably the possible LULCC at the watershed level considering the dominant LULC of the area (Wakjira et al., 2016). LULCC is among the challenges to implement IWRM (Yericho and Mulugeta, 2019). Therefore, having clear insight on LULCC and its impact on hydrologic components specifically streamflow has its contribution to implement IWRM at a watershed level as well as at basin level. This enables local government and policymakers to formulate and implement effective and appropriate response strategies to minimize undesirable effects of future LULCC (national workshop in IWRM in Gibe-Omo Basin, 2011)

Moreover, the study presents a method to quantify LULC change and its impact on streamflow. This was achieved through a method that combines the hydrological model (SWAT) to simulate the hydrological processes, GIS, and remote sensing techniques to analyze the land use land cover change.

2. LITERATURE REVIEW

2.1.LULC definition and concept

According to (Di Gregorio and Jansen, 2000) Land-cover refers to the observed biophysical cover on the earth's surface, including water bodies, vegetation, soil, and hard surfaces. Land-use is the exploitation or utilization of the land by human activities for settlements, agriculture, forestry, and other activities. LULC change is the shift in intent and/or management that constitutes LULC.

LULC change is commonly grouped into two broad categories: conversion and modification (Meyer and Turner, 1994). Conversion is defined as a change from one cover or use category to another (for example from forest to grassland). Modification, on the other hand, represents a change within one land use or land cover category (for example from rain-fed cultivated area to irrigated cultivated area) due to changes in its physical or functional attributes. These changes in LULC systems have important environmental consequences through their impacts on soil and water, biodiversity, and microclimate (Lambin et al., 2003).

2.2. Causes of LULCC

LULC changes are complex processes that arise from modifications in the land-cover to land conversion process. According to Lambin et al., (2002), LULCC is driven by the interaction in space and time between biophysical and human dimensions. According to Gereta et al., (2001) throughout the entire history of mankind, intense human utilization of land resources has resulted in significant changes in LULC. Since the era of industrialization and rapid population growth, LULC change phenomena have strongly accelerated in many regions. There is a significant statistical correlation between population growth and LULC conversion in most African, Asian, and Latin American countries (Meyer and Turner, 1994). In most developing countries like Ethiopia, population growth has been a dominant cause of LULC change than other forces (Sage, 1994). Due to the increasing demands of food production, agricultural lands

are expanding at the cost of natural vegetation and grasslands (Lambin et al., 2003). Expansion and intensification of agricultural lands, development of urban areas, and the need of extracting timber and other products are accelerating over time to meet the needs of an increasing population.

2.3. LULCC in Ethiopia

The land in Ethiopia is used to grow crops, trees, animals for food, as building sites for houses and roads, or recreational purposes. The researches that have been conducted in different parts of Ethiopia have shown that there was considerable LULCC in the country. For example, Kassa, (2003) in his study reported that in southern Wollo the decline of natural forests and grazing lands due to conversion to croplands. Gebrehiwet, (2004), in Yerer mountain, and Hadgu, (2008) in Tigray, both have reported similar result that decline of natural forest due to expansion of cropland. Ashebir, et al., (2017) studied LULCC and its effects on the landscape of the Abaya-Chamo basin. The Author reported a rapid reduction of shrubland (28.82%), Natural grassland (33.13%), and an increase in arable land (59.15% from 1985-2010. Most of these studies indicated that croplands have expanded at the expense of natural vegetation including forests and shrublands. All studies showed that there is a considerable change in land cover and land-use change in Ethiopia. Population growth has a paramount impact on the environment. Population pressure has been found to harm Riverine vegetation, scrublands, and forests in the Kalu district (Tekle and Hedlund, 2000).

Deme watershed is located on the middle east edge of the Omo-Gibe river basin. Few studies have been conducted regarding LULCC's impact on hydrology at the watershed level in the Omo-Gibe river basin. For instance, Wakjira et al. (2016) studied the effect of LULC change on the hydrologic process of the Gilgel-Gibe catchment. This study reported that the catchment has experienced LULCC from 1987 to 2010. Another study was also conducted in the Gojeb catchment under the title of LULCCs and their drivers in the Gojeb catchment (Melku et al.,

2020). Melaku, et al., (2020), reported that the major change was the expansion of cropland at the expenses of other LULC at the rate of 29.56% in 1978, 38.91% in 1987, 46.62% in 2001, and 52.74% in 2015. Mamuye et al., (2020) reported similar findings in the upper Gidabo watershed; the authors found that agricultural and urban settlement increased by 59.8% and 28.7% respectively from 1985 to 2018. Yericho and Mulugeta (2019) reported that LULCC was one of the challenges which hinder the implementation of IWREM in their study of challenges and opportunities for implementation of IWREM in the Omo-Gibe basin. LULCC studies were absent in the Deme catchment.

2.4. Image classification and LULCC detection methods

From raw remotely sensed digital satellite data, different classes or themes, usually LULC categories are extracted by the process of image classification (Weng, 2012). With the availability of historical remote sensing data, the reduction in data cost, and increased resolution from satellite platforms, remote sensing technology appears ready to make an even greater impact on monitoring LULCC. LULCC can be analyzed over a period using Landsat sensors such as Landsat Multi-Spectral Scanner (MSS) data and Landsat Thematic Mapper (TM) data by image classification techniques (Webister, 2010). Since 1972, Landsat satellites have provided repetitive, synoptic, global coverage of medium-resolution multispectral imageries. Their long history and reliability have made them a popular source for documenting changes in LULC over time (Turner et al., 2003). Image classification using remote sensing has attracted the attention of the research community (Lu and Weng, 2007).

According to Bireda, (2015), there are two primary types of pixel-based classification algorithms applied to remotely sensed data: unsupervised and supervised. Unsupervised classification is an automated classification method that creates a thematic raster layer from remotely sensed data by letting the software identify statistical patterns in the data without using any ground truth data (Lillesand et al., 2004). Whereas in the case of supervised image

classification the analyst has previous knowledge about pixels to generate representative (ground truth) parameters for each land cover class of interest. The Maximum Likelihood classification, under the category of supervised classification, is the most widely, used per-pixel method by taking into account spectral information of LULC classes (Qian et al., 2007).

LULCC detection can be defined as the process of identifying differences in the state of objects or phenomena by observing them at different times by using the remote sensing method. Principally, it also involves the ability to quantify temporal applications of remotely-sensed data obtained from Earth-orbiting satellites (Singh, 1989). Some approaches have emerged and applied in various studies to determine the spatial extent of LULCCs. For instance, Deer (1995) classified it into three categories such as pixel-based, feature-based, and object-based change. According to Lu et al., (2004) change detection methods classified into post-classification comparison, spectral-temporal combined analysis, expectation-maximization algorithm change detection, hybrid change detection. The selection depends on knowledge of the algorithms and characteristics feature of the study area (Elnazier et al., 2004). Among some change detection methods, post-classification comparison is used in this research for its simplicity and suitability to detect LULCC. In post-classification approaches two images from different dates are classified and labeled; then the area of changes extracted through the direct comparison of the classification results (Jensen, 2005; Lunetta and Elvidge, 1999).

2.5. Impact of LULCC on Streamflow

LULC plays a key role in controlling the hydrologic response of watersheds in several important ways. Changes in LULC can lead to significant changes in leaf area index, evapotranspiration (Mao and Cherkauer, 2009), soil moisture content and infiltration capacity (Fu et al., 2000; Costa et al., 2003), surface and subsurface flow regimes including baseflow contributions to streams (Tu, 2009) and groundwater recharge, surface roughness (Feddema et al., 2005), runoff (Burch et al., 1987), as well as soil erosion through complex interactions

among vegetation, soils, geology, terrain, and climate processes. Furthermore, LULC modifications can also affect flood frequency and magnitude (Ward et al., 2008; Remo et al., 2009; Benito et al., 2010; Qiu et al., 2010).

Therefore, LULC can affect both the degree of infiltration and runoff following rainfall events and rates of evaporation. Water that flows, both above and below ground can be affected by LULC properties. This evidence indicates that LULC is important determinates of the water supply on its transit through a landscape. Studies that have assessed the impact of LULC change on global terrestrial hydrology, generally, find decreased evapotranspiration and increased annual streamflow. Comparing potential (i.e., natural) to actual (present-day) vegetation, Gordon et al., (2005) suggested that decreased evapotranspiration due to deforestation is larger than the increase in evapotranspiration due to irrigation when globally averaged. Piao et al., (2007) emphasized that the observed increase in runoff over the 20th century was not only due to climate change, but that LULC change was equally important. Both surface runoff and groundwater flow are significantly affected by types of LULC (Abebe, 2005).

Numerous studies have been conducted to investigate the impact of LULCC on stream flows which ended up exhibiting the causes for streamflow changes is due to LULCC. Tan et al., (2010) studied the impact of LULCC on Johor river hydrology in Malaysia and conclude that LULC led to increased annual streamflow. A study on LULCC impact on streamflow by Mango et al., (2010) in the Upper Mara watershed revealed that the conversion of forest to agriculture decreased the dry season flow which resulted in aggravating water scarcity during low flows. Impact of LULCC and climate effects on streamflow in Chinese Loes Plateau LULCC has estimated to have 63.5% impact whereas climate change accounted for 36.48% (Hao et al., 2019). This study also reported that streamflow has decreased by -0.46mm/year due to continuously implemented land restoration action in the Loes Plateau by the Chinese government. Mamuye et al., (2020) LULCC decreased streamflow during the dry season and

increased streamflow during the wet season by 12.7% and 5.6%. respectively in the upper Gidabo watershed. Another study in Melka-Kunture reported that expansion of agricultural land correspondingly the increase of streamflow in the main rainy season and decrease during the driest season (Yitae and Van Lnnen, 2015). These all pieces of literature have sowed that there is streamflow and LULC has a strong relationship. Assessing the impact of LULCC on the hydrology of watershed in Gilgel-Abay watershed, in the Lake Tana basin also came up with similar findings (Asmamaw, 2013). The wet season streamflow in Gilgel Abay has increased by 16.26m^3/sec and decreased by 5.41m^3/sec in the dry season.

2.6. Hydrologic model

A watershed hydrology model is an assemblage of mathematical descriptions of components of the hydrologic cycle. The model structure and architecture are determined by the objective for which the model is built (Singh and Woolhiser, 2002). Cunderlik, (2003) classified models based on process description, the hydrological models can be classified into three main categories (i.e. Lumped, distributed, and semi-distributed models). For this study semi-distributed models are selected because their structure is more physically-based than the structure of the lumped model, and they are less demanding on input data than fully distributed models.

Recently, hydrological simulation models including SWAT, MIKE-SHE, HEC-HMS, and others have been developed partly to quantify the influence of change in LULC and management practices on the hydrologic cycle. Moreover, with the development of Geographic Information Systems (GIS) and remote sensing method, the hydrological catchments models have been more physically based and distributed to enumerate various interactive hydrological processes considering spatial heterogeneity (Mohan and Shrestha, 2000). Different semi-distributed hydrologic models were reviewed in Table 2-1.

Table 2-1. Model review table

Model type	SWAT	HSPF	HEC-HMS	HBV
description	Semi-distributed Physically-based long-term	Semi-distributed conceptual model	Semi-distributed Physically-based	Semi-distributed conceptual model
Model objective	predict the impact of land management practices on water and sediment	Simulates watershed hydrology, and sediment-chemical interactions	Simulate the rainfall-runoff process of dendritic watersheds	Simulate rainfall-runoff process and floods
Temporal scale	Daily	Flexible	Daily/monthly	Day/monthly
Process modelled	Continuous	Continuous & event	Continuous & event	Continuous & event
Runoff on overland	Runoff volume using CN and flow peak using Rational formula.	Chezy-Manning equation.	Clark‘s, Snyder‘s, SCS UHs, ModClark Kinematic wave	Uses response function to transform excess rainfall to runoff
Evapotranspiration	Hargreaves, Priestley-Taylor & Penman	Hamon, Jensen methods	Monthly average	Monthly average
Management practice	Agricultural management, Tillage, irrigation, etc	Agricultural management, irrigation	Account human impact on runoff	Different management practices
Reference	Neitsch et al. (2005)	Bicknell et al. (2001)	US-ACE (2001)	SHMI (2003)

2.7.Model selection

Different hydrological models simulate the LULCC effects on hydrology and sediment yield of the watershed. Several models may be capable of describing the same process. Different

models were used to assess the impact of LULCC impact on the streamflow of rivers some of them are reviewed in this literature section 2.7.

For instance, the likely LULC impacts on the hydrology of the Melka Kuntrie sub-basin in the Upper Awash River Basin have been evaluated using the semi-distributed HBV (Yitea and Van Lanen, 2015). TOPMODEL approach was applied by Webster, (2010) to simulate streamflow to assess the hydrologic impacts of LULC in the upper Gilgel Abay river basin. Topmodel can be used in the catchment with shallow soil depth and moderate topography (Gayathri 2015). In modeling of Gumara watershed (in Lake Tana basin), Awulachew et al., (2008) indicated that streamflow and sediment yield simulated with SWAT were accurate. Tekle, (2010) through modeling of Bilate watershed also indicated that SWAT Model was able to simulate streamflow reasonably accurately. Moreover, with the development of Geographic Information Systems (GIS) and remote sensing method, the hydrological models have been more physically based and distributed to enumerate various interactive hydrological processes considering spatial heterogeneity.

For the accomplishment of objectives of LULC change and impacts on streamflow of Deme catchment the following selection criteria were considered for selecting a type of model to be used:

- SWAT model predicts the output in an acceptable range to meet the objective of the study.
- Availability of input data.
- Technical support: What documentation is available about the model, Ease-of-use, and it is readily and freely available.

Based on the above selection criteria SWAT model was selected for detailed analysis and investigation of LULC change effects on streamflow of Deme catchment.

2.8. Application of SWAT model worldwide

The SWAT model has a good reputation for best use in agricultural watersheds and its uses have been successfully calibrated and validated in many areas of the USA and other continents (Ndomba, 2002; Tripathi et al., 2003). The studies indicated that the SWAT model is capable of simulating the hydrological process and erosion/sediment yield from complex and data-poor watersheds with reasonable model performance statistical values. The study by Shimaa, (2015) is used by integrating the Arc SWAT interface with Arc GIS software to model the hydrology of Simly dam watershed area. Shimaa, (2015) did Manual calibration first on annual basis followed by a monthly basis. The calibration and validation of the model produced good simulation results. The efficiency of the model has been tested by the coefficient of determination, Nash Sutcliffe Efficiency (NSE) in addition to another two recommended static coefficients: Percent Bias and RMSE observation standard deviation ratio.

However, Cibin et al., (2010) indicated that SWAT model parameters show varying sensitivity in different years of simulation suggesting the requirement for dynamic updating of parameters during the simulation. The sensitivity of parameters during various flow regimes (low, medium, and high flow) is also found to be uneven, which suggests the significance of a multi-criteria approach for the calibration of the model.

2.9. Application of SWAT model in Ethiopia

The SWAT model application was calibrated and validated in some parts of Ethiopia, frequently in the Blue Nile basin. Through modeling of Gumara watershed, in Lake Tana basin, Awulachew et al., (2008) indicated that streamflow and sediment yield simulated with SWAT were reasonably accurate. Setegn et al., (2008) reported that the SWAT model was successfully calibrated and validated. This study also reported that the model produced reliable estimates of streamflow and sediment yield from the Lake Tana basin. The SWAT model is also used in other parts of Ethiopia.

The other study by Kidane and Bogale, (2017) in Tekeze Dam watershed, northern Ethiopia, reported that the applicability of the SWAT model in simulating sediment discharge and streamflow dynamics of Tekeze Dam catchment. Ayana et al., (2014) used the SWAT model in the Fincha watershed, the Blue Nile to predict the effects of land use and management practices on runoff and sediment yields. The model gave a satisfactory estimation of runoff and sediment yield as depicted from the calibrated results. A physical-based, semi-distributed hydrological model, SWAT was again used to simulate LULC effects on the hydrological response of the Didessa sub-basin. The performance of the SWAT model was evaluated through sensitivity analysis, calibration, and validation. Both the calibration and validation result shows good agreement between observed and simulated streamflow with NSE and R^2 values of 0.7 and 0.79 respectively. (Tesfa et al., 2016).

SWAT model was used to examine the impact of LULC changes on the hydrological process of the Gilgel gibe catchment in the Omo-Gibe basin. The R^2 and NSE values were used to examine model performance and the result indicates 0.84 and 0.90 to R^2 and 0.58 and 0.62 to NSE during calibration and validation respectively (Wakjira et al., 2016). This all literature has shown that the performance of SWAT should be carried out through calibration and validation before applying it to a particular watershed or river basin. However, the SWAT model was not calibrated and validated in the Deme catchment yet. The performance evaluation formula and its acceptable range to evaluate the model was described in Table 2-2.

Table 2-2. Performance evaluation formula, values, and performance classification.

Statistical criteria	Values	Performance classification
$NSE = 1 - [\frac{\sum(Qo - Qs)^2}{\sum(Qo - Mean.Qo)^2}]$	0.75 to 1	Very good
	0.65 to0.75	good
	0.5 to 0.65	satisfactory
	0.4 to 0.5	acceptable
	< 0.4	unsatisfactory
$PBIAS = [\frac{\sum(Qo - Qs)}{\sum Qo}]$	<±1	Very good
	±10 to ±15	good
	±15 to ±25	satisfactory
	≥±25	unsatisfactory
$R^2 = \frac{[\sum(Qo - mean.Qo)(Qs - mean.Qs)]^2}{\sum(Qo - mean.Qo)2 \ \sum(Qs - mean.Qs)^2}$	>0.6	acceptable

(Source: Tolera, 2018, A Thesis Submitted to the School of Graduate Studies of Addis Ababa University).

2.10. Strength and weakness of SWAT model

There are many opportunities outside the SWAT model that provide a unique possibility for growth and change of the model in the future. Numerous environmental problems due to land use policy resulted around the world encouraging the use of the models like SWAT. In Tables 2-3, the weakness and strengths of the SWAT model were elaborated clearly.

Table 2-3. Review on strength and weakness of SWAT model.

The Strength of SWAT model	The Weakness of SWAT model
➢ The SWAT model is easily available on-line ➢ It is capable of yearly, monthly, and daily simulation over a long period. ➢ It enables to study of water quantity, water quality, LULCC, and Climate change. ➢ It is a comprehensive model integrating surface land and channel environmental processes. ➢ It has a flexible framework that allows simulation of Agro-environmental measures and best management practices. ➢ SWAT model has supportive tools like SWAT-CUP, SWAT editor-interface, MWSWAT interface	➢ The SWAT model uses equations that have parameters that are not directly measured using data, for example, CN-equation. ➢ Sensitivity analysis, manual calibration, and auto-calibration tools in the SWAT model are time demanding. ➢ A wide range of different data needs to be obtained to run the model and numerous parameters needed to be modified during the calibration.

(Source: Matjaz, G., and Marina, P. (2012). Strengths, weaknesses, opportunities, and threats of catchment modeling SWAT model).

2.11. Hydrologic and meteorological data analysis methods

A lengthy rainfall data series plays a major role in all water-related studies. Consistency and continuity of rainfall data series are very important for obtaining reliable results from such studies. However, these rainfall data series very often contain gaps or missing values due to various reasons such as the absence of observers, problems with measuring devices, loss of records, etc. The use of a rainfall data series with missing values may critically influence the statistical power and accuracy of a study (Caldera et al., 2016).

Estimation of missing data is more important in mountain and forest regions where meteorological stations are scarce, and the observed data are influenced by topography and the forest microclimate. The techniques of missing data estimation can be grouped in empirical methods, statistical methods, and function fitting (Xia et al., 1999).

The empirical methods include simple arithmetic averaging, inverse distance interpolation (ID), and ratio and difference technique The statistical methods include multiple regression analysis (REG), principle component analysis and cluster analysis, the Kriging method, and optimal interpolation. Most of these methods derive the missing values using observations from neighboring stations. Selecting appropriate methods for estimating missing precipitation data may improve the accuracy of hydrological models.

De Silva et al., (2007) used the aerial precipitation ratio method, the arithmetic mean method, the normal ratio (NR) method, and the inverse distance method to estimate missing rainfall data. The NR method was found to be the most accurate. The arithmetic mean method and the aerial precipitation ratio method were most appropriate for the wet zone. According to Caldera et al., 2016 to obtain accurate results from the Multiple Linear Regression method and the Weighted Linear Regression method, it is necessary to have a set of neighboring stations that have fairly high correlation coefficients with the target station. And also they stated in their result that for stations that have relatively low correlation coefficients with the neighboring

stations, the Inverse Distance Squared method and the Normal Ratio method outperformed well.

As the literature review shows that the best method for estimating missing rainfall data can vary for different areas depending on their rainfall patterns and spatial distributions and availability of the neighboring station. For this study arithmetic and normal ratio, the method is selected as per the requirement of the condition.

3. MATERIALS AND METHODS

3.1.Study area description

3.1.1. Location

The study area Deme catchment is one of the sub-catchment in the middle Omo gibe river basin. This catchment is located in the SNNPR State of Ethiopia between the southwest of Wolaita and northeast of Gamo administrative zones. The outlet of the catchment lies $6^0$38'N, Latitude, and $37^0$31'E longitude. The geographical location of the study area was $6^0$15'N, $37^0$25'E in southwest, $6^0$58'N, $37^0$25'E in northwest, 6058'N, $37^0$48'E in northeast, and $6^0$15'E, $37^0$48'E. in southeast. The Deme catchment starts from the highland part of northern Zara woreda and the southwest part of Wolaita-Sodo town. The total area of the Deme catchment, upstream of the gauging station of Oratalem is estimated at 1111.723km^2. The boundary of the study area was clearly shown in figure 3.1.

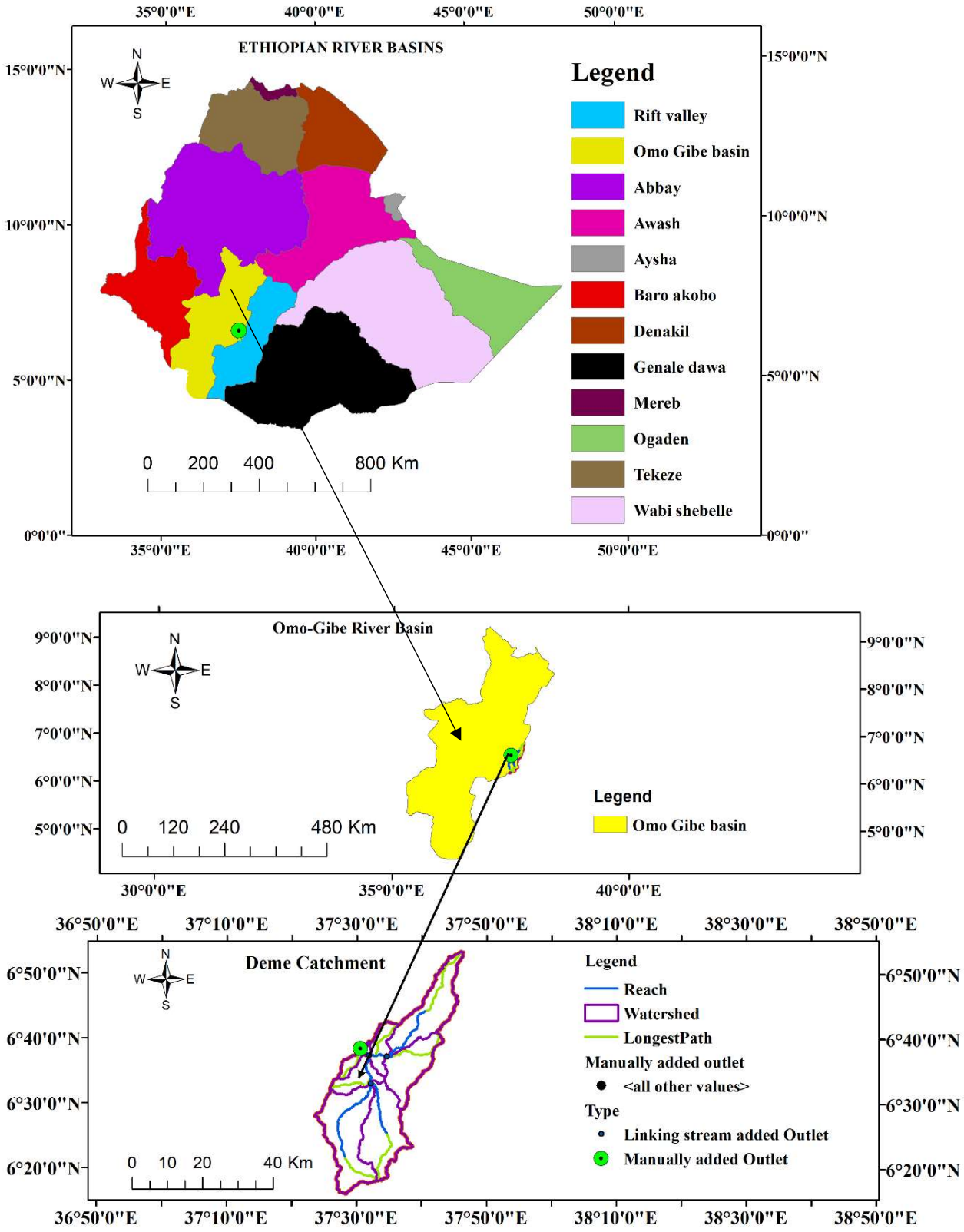

Figure 3-1. Study area location.

3.1.2. The climate of the study area

The climate of Ethiopia can be classified in different ways. The most commonly used systems are the traditional and agro-ecological zone. According to traditional classification, there are five climatic zones namely wurch (cold climate, altitude>3000masl), Dega (temperate like climate, with altitude 2500-3000masl), Woine dega (warm with altitude1500-2500), Kola (hot and arid with altitude<1500masl), and Bereha (hot and hyper-arid type) climates (NMSA., 2001). The study area falls within 'Dega' (temperate), 'Woina Dega' (sub-tropical), and 'Kolla' (tropical) i.e. 55%, 35%, and 10% climatic zones respectively (Sintayehu, 2016). Classification for rainfall regimes shows the presence of a bimodal rainfall pattern in the study area. The first round of rain occurs in March, April, and May and the second round of rain occurs from June, July, and August. The rainfall distribution varies from year to year and across seasons. The study area receives mean annual rainfall between 1374mm to 1197mm as studied from the representative stations of the study area. (Sodo zuria, Gesuba, Danna 2, and Dinke metrological stations). The mean monthly temperature of the study area was shown in figure 3-2.

Table 3-1. Mean monthly rainfall (mm) data for 30 years from 1989 to 2018.

Name	Jan	Feb	Mar	Apr	May	Jun	Jul	Aug	Sep	Oct	Nov	Dec
Danna 2	37.4	28.2	92.6	151.7	175.5	156.2	181.7	190.5	157.5	113.6	53.5	28.4
Dinke	30.5	46.1	101.4	146.0	183.9	131.2	159.8	171.4	151.5	73.8	28.7	25.3
Gesuba	30.0	33.7	76.7	140.1	193.7	113.2	163.7	164.9	111.6	99.4	42.6	27.7
Wolaita Sodo	30.3	41.6	80.4	169.2	186.8	143.2	181.4	181.0	113.9	100.9	66.5	37.1

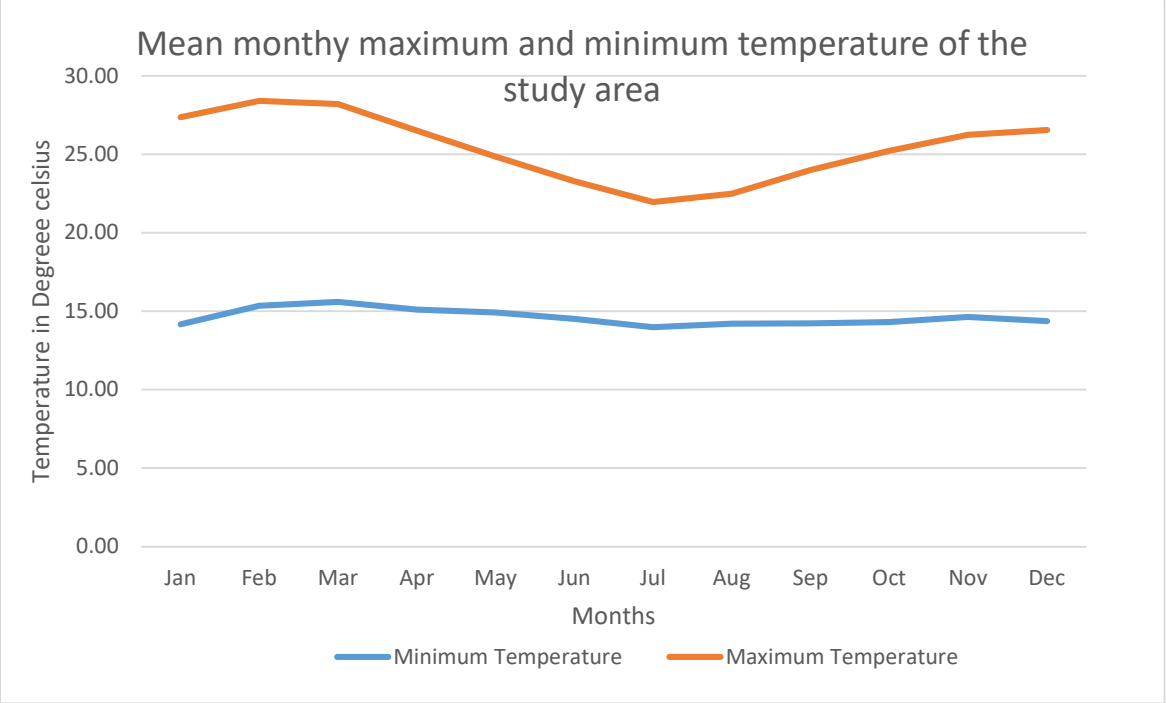

Figure 3-2. Mean monthly Minimum and maximum temperature calculated from 1989-2018.

3.1.3. Topography

Elevation of Deme catchment ranges from 1140m to 3488masl as clearly shown in figure 3-3. Starting from Selamber town (Kucha woreda) to the outlet of the catchment (i.e. Western and central part of the watershed) is characterized by a flat landscape. Extending from the Southwest of Wolaita town to Selamber (Kucha woreda) the catchment is characterized by an undulating plain and Gently sloping landscape. The Northern tip of wolaita-Sodo town and the southern tip (the highland area of Zara woreda) of the catchment is characterized by hilly to the mountainous landscape.

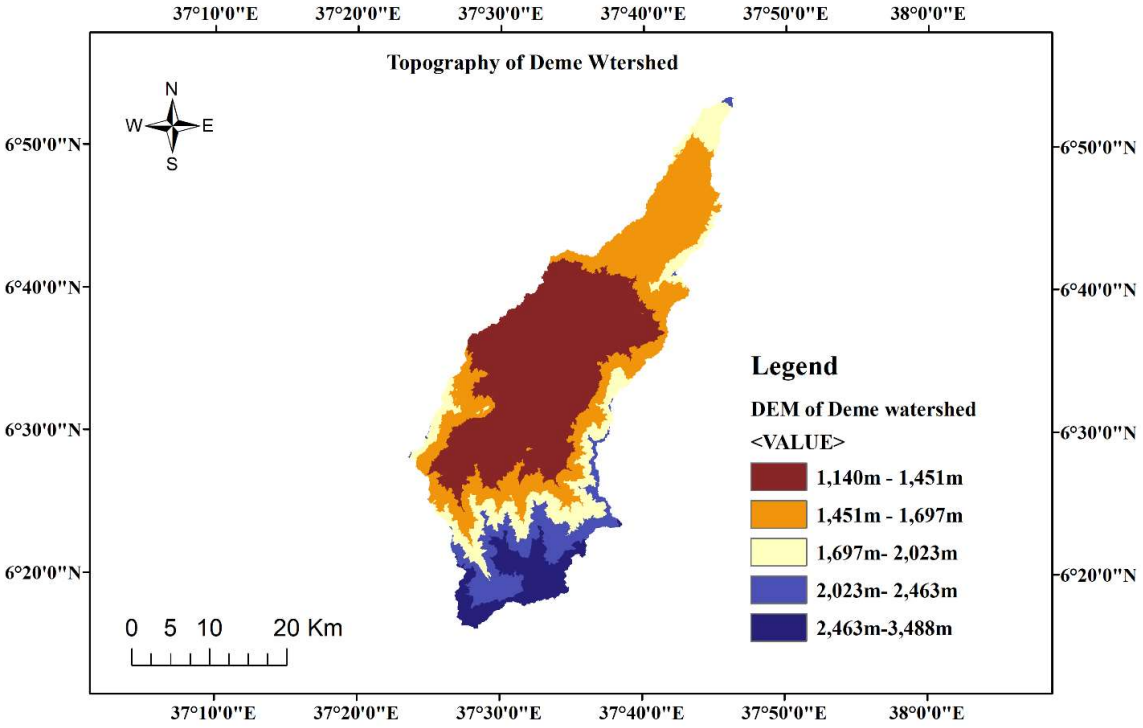

Figure 3-3. Topography of the study area

3.1.4. Vegetation cover and soil of the study area

Due to a high altitudinal variation, the study area is characterized by diverse agro-climate, soil, and vegetation cover. The eastern catchment boundary of the Omo-Gibe basin has the most densely populated and intensively farmed areas in the basin (Dereje, 2015). Hence Deme catchment is in the middle east of the basin, the land use pattern of the watershed is intensively cultivated and different crops are grown. Deforested areas are now confined to areas steep and inaccessible to farm (Richard woodroof and associates, 1996). The identified LULC in the Deme catchment is agriculture, bushland, mixed forest, built-up area, and Grassland. According to the FAO/UNESCO soil classification system, the study area comprises five soil types, such as Humic alisol, Lithic leptosol, Chromic Luvisol, Humic Nitisol, and Eutric vertisol. The shapefile of soil data was taken from the ministry of water, irrigation, and electricity of Ethiopia.

3.2. Estimation of land use land cover change

3.2.1. Data collection for estimation of LULCC

Satellite data for the year 1999, 2010, and 2018 were obtained from the USGS website. The aforementioned satellite image was selected based on historic event. For instance, before 1999 the study area was administrated by WoGaGoDa. This administration was decentralized in to Wolaita, Gamo-Gofa and Dawro by the ruling party of EPRDF in 2000 (Data, 2006). Therefore, the year 1999 was used as the base line to analyse the LULCC in the study area. Landsat 5 TM for 2010, Landsat 7 ETM+ for 1999, and Landsat 8 OLI for 2018 were used. The cloud-free image of the study area was downloaded in a zipped file from the website of USGS. The study area was between the path and rows of 1969/055 and 1966/056. To avoid seasonal variation in vegetation, pattern the image data were acquired in the same season as much as possible. The detail for the satellite data were described in table 3-2.

Table 3-2. Description for Landsat image used for the study.

Sensor	Name	Multispectral band	Thermal band	Path	Row	Acquisition date	Spatial resolution (m)	Producer
ETM+	Landsat 7	1 to 5 and 7	6	169	055	26/12/1999	30*30	USGS
				169	056	26/12/1999	30*30	USGS
TM	Landsat 5	1 to 5 and 7	6	169	055	30/01/2010	30*30	USGS
				169	056	30/01/2010	30*30	USGS
OLI	Landsat 8	1 to 7 and 9	10 and 11	169	055	23/01/2018	30*30	USGS
				169	056	23/01/2018	30*30	USGS

3.2.2. Image classification

Firstly, the number and types of the existing LULC classes in the Deme catchment were identified. The existing LULC clas was identified by looking research papers which were done around the study area as well as in Omo-Gibe river basin. For example Wakjira (2016), in Gilgel gibe catchment of Omo-gibe basin reported the LULC as Forest land, built-up area, agricultural land, and Range land. Tadele (2007), in Hare watershed near to Deme catchment reported the LULC as Farm Land, Forest land, Shrub land, Grass land. Derege (2015), in Omo-Gibe basin reported that cultivated land, Bush land, Grass land, forest land, and built up area were among the 13 LULC classes identified by the auther. Following the identification of LULC classes in the study area, image classification was carried out. The identified LULC classes were described in Table 3-3.

Table 3-3. Description of LULC classes.

LULC types	Descriptions
Agricultural land	Areas of land plowed/prepared for growing rain-fed or irrigated crops. This category includes areas currently under crop, fallow, and land under preparation. The class may also include small interfiled cover types such as grass strips, hedges, and small windbreaks.
shrub land	Areas covered with shrub, bushes, and small trees, with little useful wood, mixed with some grasses.
Grass Land	Areas covered with mainly natural pastures rangeland, grass-like, and other small-sized plant species.
Built-up areas	Areas occupied by house buildings such as residential, commercial, industrial, and mixed urban areas.
Forest	Areas covered with dense trees, which include both eucalyptus and coniferous trees.

(Source; Tadele (2007). Impact of Land Use/Cover Change On Stream Flow: The Case of Hare River. Arbaminch University. Ph.D. Dissertation.)

Image classification brings pixels together to represent a specified LULC class. The task of extracting information classes from multiband raster images was done using USGS satellite images for selected years (1999,2010 and 2018). In the first phase, image preprocessing techniques were carried out first. This was layer stacking, mosaic an image, and sub-setting an image. To analyze remotely sensed images, different images representing different bands were stacked. Layer stacking allows the different combinations of RGB to be shown in the view. During layer stacking, all bands were stacked except the thermal band for all Landsat images. Mosaicking image was used because the study area has lied over two swaths i.e. path/row of 169/055 and 169/056. After mosaicking, a sub-setting of the portion of the study area was carried out.

After preprocessing finished, image classification was done. For this study, the LULC map was produced based on the pixel-based supervised Maximum likelihood classification. Selecting the training sites which are typically representative of the LULC classes was done by using google earth. Landsat image of google earth was used to take the area of training for all Landsat images. The Year and date of the google earth image used for the training area were set similar to the Landsat images used for classification. The Landsat image of google earth was used to take the area of training for all imageries (1999, 2010, and 2018). Table 3-4, describes the number of areas of training used for each LULC map, and the type and date of the image from google earth used for the classification. To do this Google earth was connected to ERDAS IMAGIN 2014 to take the area of training for all satellite images. The number of training sites should be at least three times the number of categories of interest (Khorram, 2013). After the training area assigned for each class classification activity was performed.

Table 3-4. Description area of training used for LULC classification.

LULC map	Area of training for AGRL	Area of training for BTUA	Area of training for FRST	Area of Training BSL	Area of training for GRL
1999	100	20	100	30	77
2010	100	22	100	38	72
2018	200	27	100	146	72

The final stage, image post-classification was then carried out. Techniques which was utilized in post-processing include recoding and accuracy assessment. Accuracy assessment of the classified images was done for verification and validation of the results. The same classes having different reflectance colors were classified individually or separately and then merged into a single class.

3.2.3. Accuracy assessment

Accuracy assessment is an important step in the image classification process. It is a process used to estimate the accuracy of image classification by comparing the classified map with a reference map (Caetano et al., 2005). Error matrix was used to derive a series of descriptive and analytical statistics for accuracy assessment (Manandhar et al., 2009). The columns of the matrix depict the number of pixels per class for the reference data, and the rows show the number of pixels per class for the classified image. From this error matrix, overall accuracy, user's and producer's accuracy were reported.

The accuracy assessment of the classified map was done by comparison of the classified image and Google Earth Imageries. Stratified random sampling was used in this study. For stratified random sampling, provides the following sample size formula (Cochran 1977). This formula was used to determine the sample size to carry out the Accuracy assessment.

$$N = \left(\frac{\sum Wi Si}{So}\right) \ldots\ldots\ldots\ldots\ldots\ldots\ldots\ldots\ldots\ldots\ldots\ldots\ldots\ldots (3.4)$$

Where Wi = is mapped proportion of the area of class i

$$Si = \sqrt{Ui} * \sqrt{(1-Ui)} \ldots\ldots\ldots\ldots\ldots\ldots\ldots\ldots\ldots\ldots (3.5)$$

So = is the standard error of estimated overall accuracy that we would like to achieve. And Ui= is for user's accuracy

For these studies, the standard error is used to be 0.01 and the user's accuracy 0.98. This finally gives 386 which is a total reference point used to do accuracy assessment for this study. Table 3-5 describes the number of reference points used for each LULC class during accuracy assessment.

Table 3-5. The description of reference points used for accuracy assessment.

LULC Map	Reference Points For AGRL.	Reference points for BTUA	Reference points for FRST	Reference points for BSL	Reference points for GRL
1999	100	10	111	107	58
2010	124	22	103	89	39
2018	141	36	78	87	44

3.2.4. LULCC detection

The process of identifying differences in the LULC of the Deme catchment was done by observing the classified images at different times (1999, 2010, and 2018). Therefore, comparisons based on three satellite images of 1999, 2010, and 2018 were made. To achieve this, the first task was developing a table showing the area, percent, and changes between the

periods of 1999-2010 and 2010-2018 measured for each LULC. Temporal change and rate of change were also computed to demonstrate the magnitude of the changes experienced.

$$Temporal\ LULCC(\%) = \frac{Area\ at\ final\ Yr. - Area\ at\ initial\ Yr.}{Area\ at\ initial\ Yr.} * 100 \ldots\ldots (3.6)$$

$$Rate\ of\ change\ = \left(\frac{Final\ Area\ at\ Final\ yr. - Area\ at\ Initial\ Yr.}{Area\ at\ initial\ Yr.} * 100\right) * 1/T \ldots\ldots (3.7)$$

Where T is the difference in time between two periods.

3.3.Analysis of the impact of LULCC on streamflow

Evaluation of the impacts of LULCC on streamflow is one of the most significant parts of this study. The study was carried out for three different years i.e. 1999,2010, and 2018. The three classified LULC maps, soil, climatic, and streamflow data values were used to evaluate the impacts of land use and land cover change on streamflow.

To evaluate the variability of streamflow due to LULCC, the three LULC maps (1999, 2010, and 2018) were used independently in the three simulations while keeping other variables constant. The study then discovered annual variation and seasonal variation of streamflow due to the LULC map of 1999, 2010, and 2018. The simulated streamflow for the three-time period (1999, 2010, and 2018) was grouped into four Ethiopian seasons (Kiremt, Belg, Bega, and Tsedey) to see the seasonal variability of streamflow. Then contributors of streamflow (SURQ, LATQ, and GWQ) flow values for each LULC map were also compared to each other.

Table 3-6. Justification on Four Ethiopian seasons

Seasons (Amharic/English	Months included	Characteristics
Kiremt/summer	June, July, and August	Heavy/main rainfall
Belg/Autumn	September, October, November	Small rainy season
Bega/winter	December, January, February	The dry season
Tsedey/spring	March, April, May	Infrequent/Occasional showery rain.

(Source; Fekadu Bekele, Ethiopian treasures, Ethiopian National Metrological Services Agency, http://ccb.colorado.edu/ijas/ijasno2/bekele.html, Addis Ababa, Ethiopia.

3.3.1. Data collection for the analysis of impact of LULCC on streamflow

Different types of data such as meteorological, hydrological, and satellite images were utilized to attain the objective of this study. These data were collected from different agencies and organizations. The DEM and satellite data were obtained from the USGS website. Soil and hydrologic data were collected from the ministry of water, irrigation, and electricity of Ethiopia. The meteorological data such as Rainfall, Temperature, humidity, and solar radiation, were obtained from the national meteorological agency of Ethiopia.

3.3.1.1.DEM data

DEM is a digital representation of a topographic surface and specifically to a raster or regular grid of spot heights. The DEM data were used to delineate the watershed, to extract information about the topography or elevation of the watershed by using the ArcGIS integrated SWAT model. For this study, 30m by 30m resolution ASTER global DEM was obtained from the USGS website.

3.3.1.2.Soil data

The soil map in raster form for the study area was obtained from the Ministry of Water, Irrigation, and Electricity of Ethiopia. This soil map of the FAO database was overlaid with the shape file of the study area to match and get the nomenclatures of the soil class of the Deme catchment. SWAT model requires physical and chemical properties of soil such as soil texture, available water content, hydraulic conductivity, bulk density, and organic carbon content for different layers of each soil type. These properties were taken from the ministry of water, Irrigation, and Electricity of Ethiopia. A new excel file containing the same column titles as the SWAT user soil table was created and those prepared soil properties were filled accordingly to use in the Arc SWAT2012 database. This prepared excel sheet was then copied to the soil database of the SWAT model. The soil map of the study area was shown in figure 3-4.

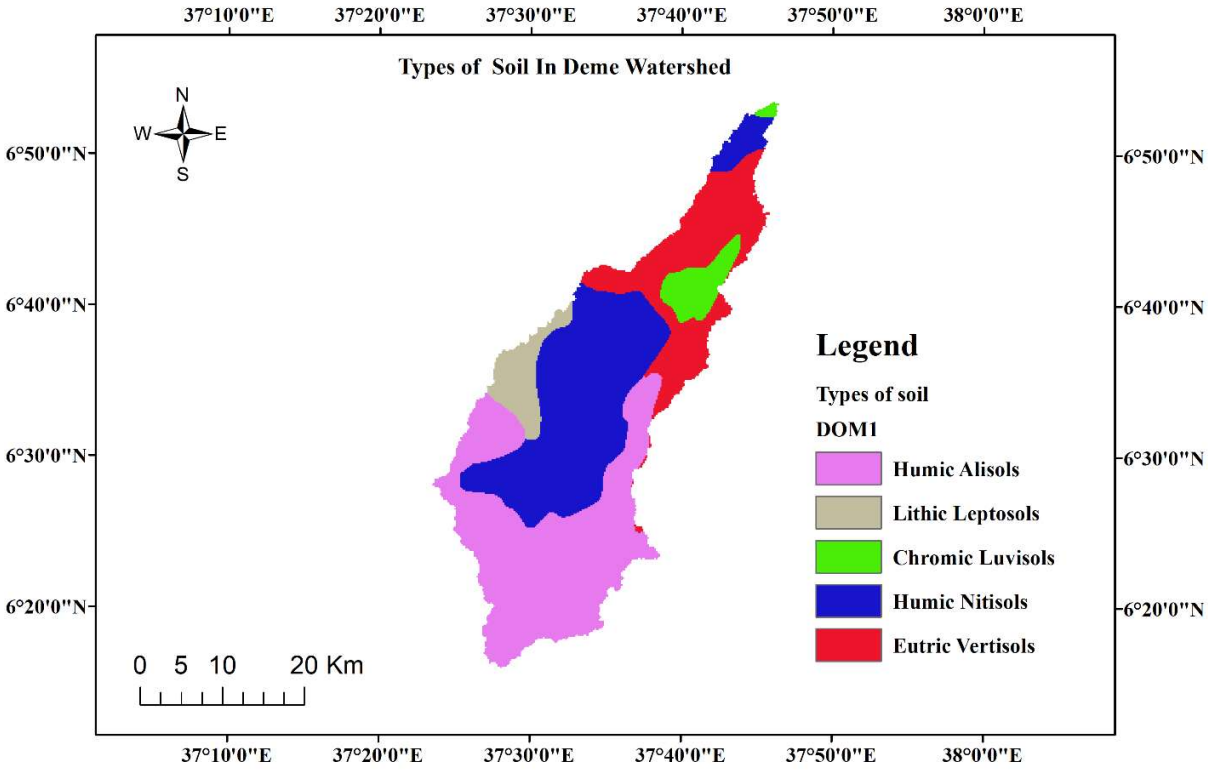

Figure 3-4. Soil map of the study area

3.3.1.3.Streamflow data

Water resource studies highly depend on streamflow data. Daily streamflow data for Deme river from 1989 to 2006 GC, from Oreta-alem station, was collected from the Ministry of Water, Irrigation, and Electricity of Ethiopia. The gauging station has good streamflow records from 1989 to 2006 GC. This data was used for calibration and validation purposes to analyze the impacts of LULCC on streamflow.

3.3.1.4.Meteorological data

The meteorological data is among the most needed parameter of the SWAT model. Input data required for SWAT simulation includes daily data of precipitation, maximum and minimum temperature, relative humidity, wind speed, and solar radiation. These data were obtained from the Ethiopian meteorology station. The weather data used were represented from four stations in the Deme catchment such as Wolaita-Sodo, Danna 2, Gesuba, and Dinke meteorological

stations. The climatic data used for this study covers from 1989 to 2018. Based on the class of the station, the number of weather variables collected varies from stations to stations. The detailed descriptions for meteorological stations were shown in Appendix. The distribution of a representative meteorological station in the watershed was shown in Figures 3-5.

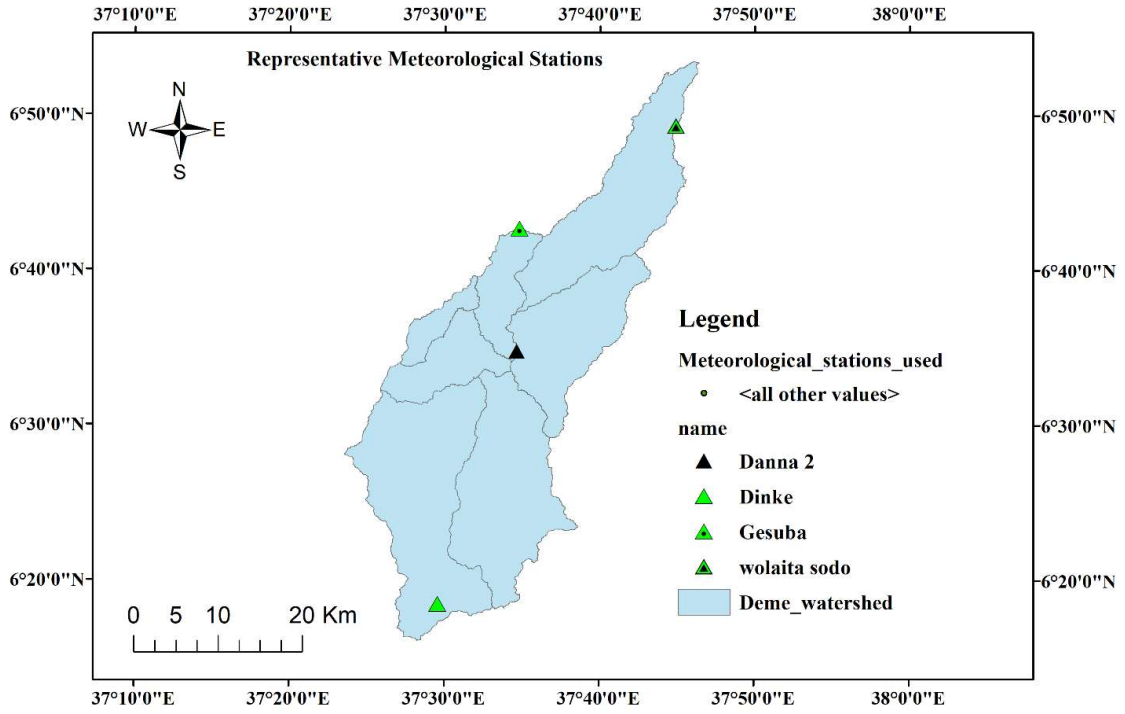

Figure 3-5. The distribution of Meteorological stations

3.3.1.5.Meteorological data analysis

I. Filling missing data

Although complete hydro-meteorological data is a pre-requisite for successful water resource planning and management, significant data sets are usually missing due to interruption of measurements caused by natural and/or human-induced factors (Subramanya, 2008). Before using the metrological record of the station, it is necessary to check the data for continuity and consistency. To do these the missing data should be filled in by using the data of the neighbor station.

The normal ratio method was conceptually simple and can be used if the total annual rainfall at the gauging station differs from the annual rainfall at the point of interest by 10% (Subramanya, 2008). The normal ratio method was used to fill the missing data of rainfall and temperature from the nearest stations for other stations for this study.

$$Px = \frac{Nx}{M} * \left[\frac{P1}{N1} + \frac{P2}{N2} + \ldots + \frac{Pm}{Nm}\right]$$

Where Px is the current rainfall value for station X,

P1, P2, and Pm are current rainfall values for the neighbor stations.

N1, N2, and Nm are the average annual precipitation for the neighbor station.

II. Homogeneity test

Rainfall data analysis is important to identify whether the rainfall stations in or around a watershed are regionally showing similar characteristics that will help for further analysis like filling missing data. Homogeneity analysis is used to identify a change in the statistical properties of the time series. The causes can be either natural or man-made. These include alterations to land use and relocation of the observation station. Therefore, to select the representative meteorological station for the analysis of areal rainfall estimation, checking the homogeneity of group stations is essential and the homogeneity of the selected gauging station's monthly rainfall records was carried out by non-dimensional parametrization.

$$i = \frac{Over\ year\ average\ monthly\ PCP\ for\ month\ i}{the\ over\ years\ average\ yearly\ PCP\ of\ station}$$

Where Pi: non-dimensional values of precipitation for a month i.

PCP: precipitation of the station

The selected stations were also plotted for comparison with each other in Figure 3-6. They showed the same model and pattern for the selected station. These assure that the selected stations were homogenous.

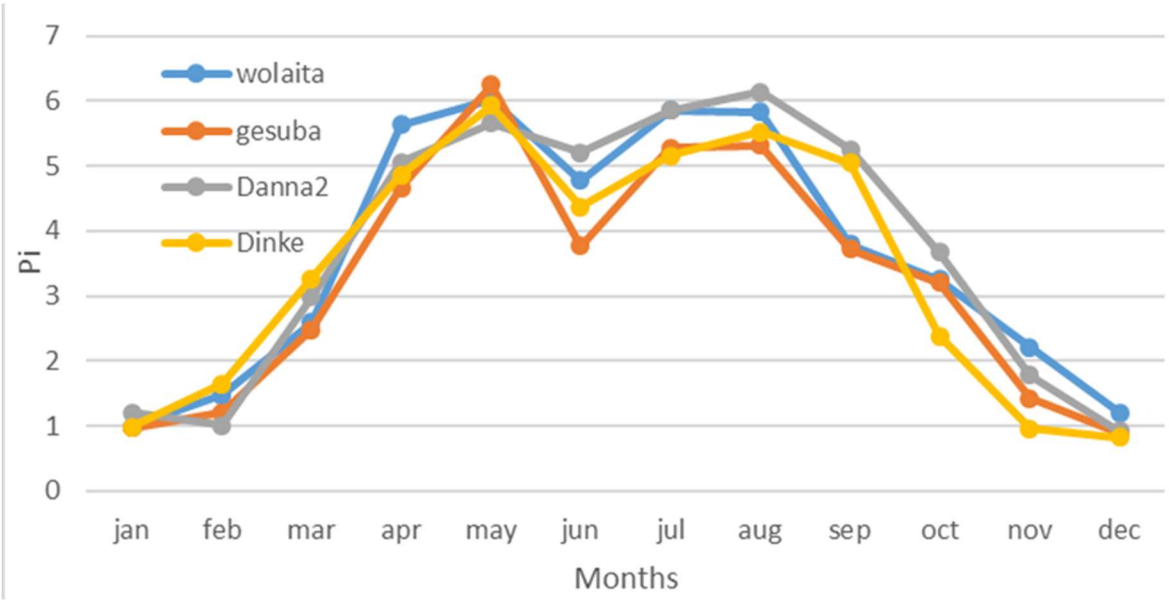

Figure 3-6. Homogeneity of the stations used for study.

III. Consistency test

A double mass curve (DMC) was used to check the consistency of rainfall for adjustment of inconsistent data. This technique is based on the principle that when each recorded data comes from the same parent sample, they are consistent.

A consistent record is one where the characteristics of the record have not changed with time. A double-mass curve is a graph of the cumulative catch at the rain gauge of interest versus the cumulative catch of one or more gauges in the region that has been subjected to similar hydro-meteorological occurrences and is known to be consistent. The double-mass curve will have a constant slope if a rainfall record of the hydro-meteorological occurrences for the record is consistent. A change in the slope of the double mass curve would suggest that an external factor has caused changes in the character of the measured values. If a change in slope is evident, then either the record needs to be adjusted with either the early or the later period of record which is not disturbed. Figure 3-7, depicted that the selected meteorological stations were consistent.

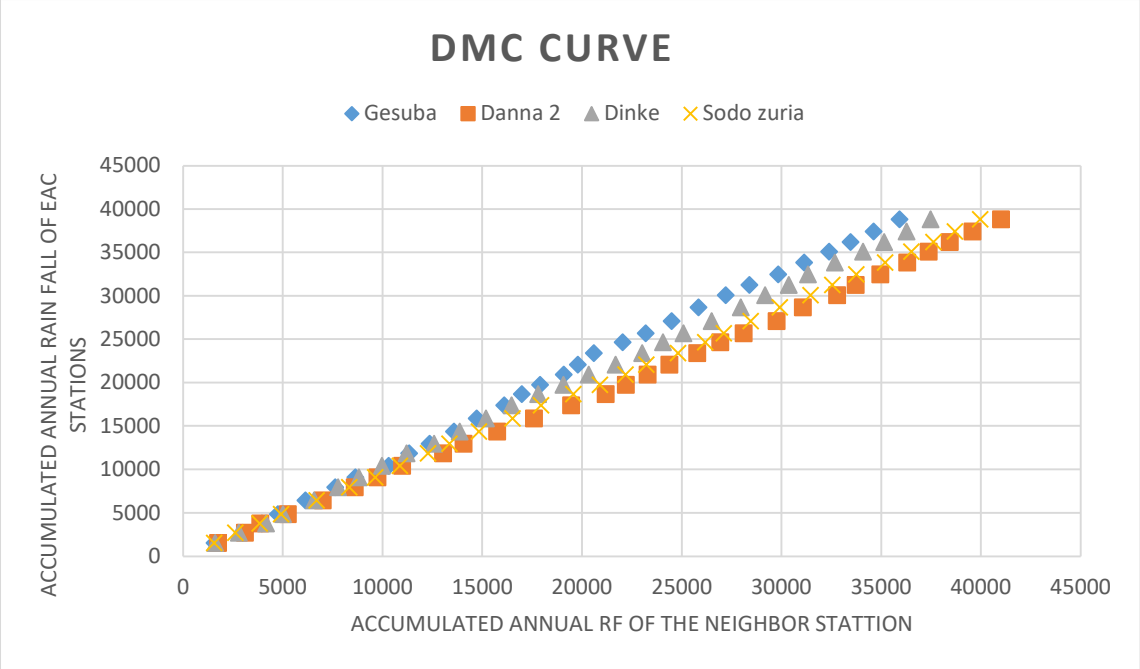

Figure 3-7. Double mass curve for consistency test

3.3.2. SWAT MODEL DESCRIPTION AND SETUP

3.3.2.1.Hydrologic equation of SWAT model

SWAT operates on daily time step climatic data and is used to predict the impact of LULC on streamflow. In the SWAT model, a catchment is divided into multiple sub-watershed, which is further divided into hydrologic response unit (HRU) which consists of homogeneous LULC, topographical, and soil characteristics. The HRU is represented as a percentage of the sub-watershed area. The water balance components of each HRU are computed on the daily time step. Water balance is the driving force behind all the processes in the SWAT model. Weather data such as daily precipitation, maximum/minimum air temperature, solar radiation, wind speed, and relative humidity are used to do the water balance by SWAT model. SWAT simulates the hydrological cycle based on the water balance equation 3.8

$$SWt = SWo + \sum_{i=1}^{t}(Rday - Qsurf - Ea - Wseep - Qgw) \quad \text{.....(3.8).}$$

Where SWt = the final soil water content (mm),

SWo = the initial soil water content on day i (mm),

t = the time (days),

Rday = the amount of precipitation on day i (mm),

Qsurf = the amount of surface runoff on day i (mm),

Ea= the amount of evapotranspiration on day i (mm),

Wseep= the amount of water entering the vadose zone from the soil profile on day i (mm),

Qgw =the amount of return flow on a day i (mm).

Surface runoff from daily rainfall is estimated using the SCS curve number method, which estimates the amount of runoff based on local LULC, soil type, and antecedent moisture condition. The watershed concentration time is based on manning's formula, considering both overland and channel flow.

I. Surface runoff

Surface runoff occurs whenever the rate of precipitation exceeds the rate of infiltration. The SCS method was used to estimate surface runoff because of the unavailability of sub-daily data for the Green &Ampt method. The SCS curve number equation is:

$$Qsurf = \frac{[Rday- \ .25S]^2}{[Rday \quad .8s]} \ldots\ldots\ldots\ldots\ldots\ldots\ldots\ldots\ldots\ldots\ldots\ldots\ldots\ldots \ (3.9)$$

In which, Qsurf is the accumulated runoff or rainfall excess (mm), Rday is the rainfall depth for the day (mm), S is the retention parameter (mm). The retention parameter is defined by the equation:

$$S = 25.4 * [\frac{100}{CN} - 10] \ldots\ldots\ldots \ (3.10).$$

Where, CN is the curve number for the day and its value is the function of land use practice, soil permeability, and soil hydrologic group.

3.3.2.2.SWAT model setup

Arc SWAT version 2012 was the extension of Arc GIS and its toolbar was added to Arc GIS10.4 for use to meet the objective of the study. SWAT project setup, watershed delineation,

and HRU analysis write input tables, edit SWAT input, and SWAT simulation were the procedures in the SWAT model setup.

I. Watershed delineation

In the SWAT project set up the project name and its file location were specified first. Then the next step was a watershed delineation. The watershed delineation was performed using 30m by 30m resolution of DEM. DEM data was projected to UTM under zone 37. After loading DEM, the stream definition was the next step. The stream definition was done by selecting the threshold area. The threshold area used to form a stream be 8000 hectares to decrease the number of sub-watersheds. Watershed delineation was more refined in the section by defining the outlet point for the whole watershed. The outlet location of the Deme catchment (Oratalem) was added manually to the defined streamline. The final step in the delineation of the watershed was the calculation of basin parameters such as geomorphic parameters and stream reach.

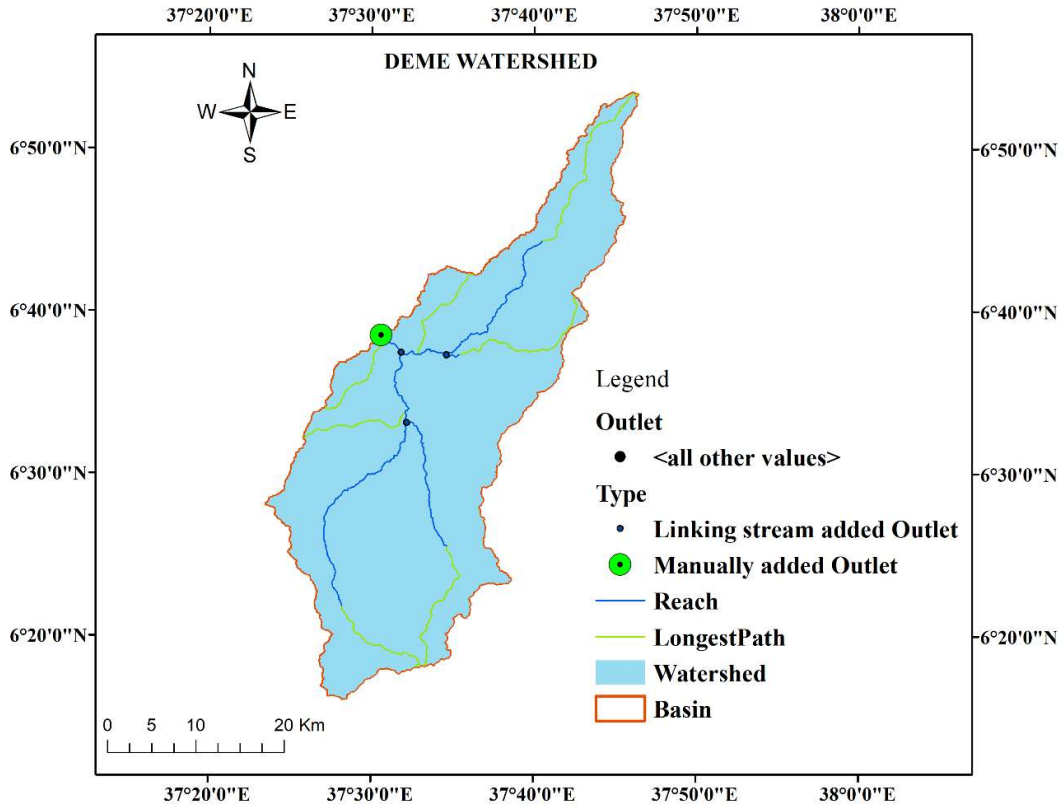

Figure 3-8. The Delineated Deme watershed.

II. Hydrologic response unit

After watershed delineation, LULC, soil, and slope characterization for watershed were performed using commands from the HRU analysis menu of the Arc SWAT toolbar. This tool was used to loading LULC and soil layers of the Deme catchment into the current project. Therefore, LULC/soil/slope combinations and distribution for the delineated Deme catchment were determined in HRU analysis. Finally, the watershed was divided into HRU which has similar soil, LULC, and slope combination.

The prepared composite LULC map and soil map were given as input to the model in this step. The lookup table containing various SWAT LULC class codes was prepared. This prepared Lookup table was linked to the SWATs LULC database. This lookup table has two columns named as value and name. The value in the lookup table corresponds to the value of LULC class in the attribute table for the classified image, and the name corresponds to the name of the LULC class which corresponds to the name in the SWAT database. This prepared lookup table is then called during LULC/Soil definition during HRU formation. Figure3-9 shows how the LULC map is linked with the Arc SWAT database.

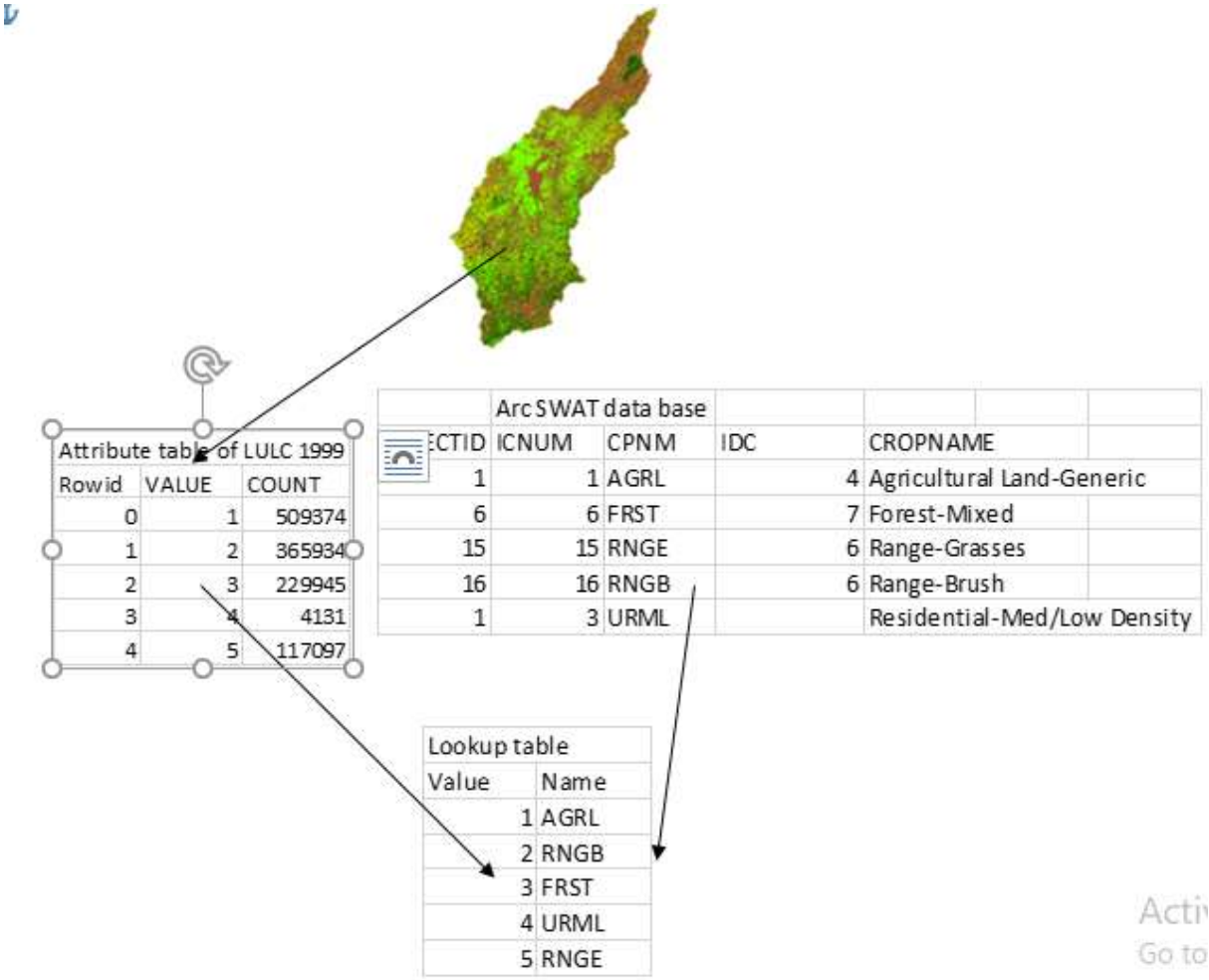

Figure 3-9. linking LULC map with Arc SWAT database.

Similarly, soil physical attributes were initially stored in the SWAT database through an interface, with relevant information required for hydrologic modeling. This Arc SWAT soil database and the soil data of the study area were linked by using a lookup table.

For defining HRU distribution, the multiple HRUs options, which create multiple HRU within each sub-watershed was chosen. The number of HRU in the watershed was controlled by the threshold value given during HRU definition. Melese, (2008) suggested that 10% LULC, 20% soil, and 10% slope give a better estimation of streamflow. Therefore, for this study 10%, 20%, and 10% threshold value was used to create LULC/soil/slope combination.

III. Write input table

After HRU analysis, the weather data to be used in the simulation was imported using the first command in the write input table menu item on the Arc SWAT toolbar. This tool helps to load weather stations located into the current project and assign weather data to the sub-watershed. The weather data definition is divided into six tabs weather generator data, rainfall data, temperature data, solar radiation data, wind speed data, and relative humidity data. Arc SWAT reads weather data from the WEGEN users database in which relevant information about climate required for hydrologic modeling was stored. The SWAT weather database, which was designed to be friendly to store and process daily weather data to be used with the SWAT project, is used to create WEGEN users. Then this prepared WEGEN user was imported to the SWAT database to use. Then for weather data definition, the weather generator data file WGEN user, rainfall data, temperature data, relative humidity data, solar radiation data, and wind speed data for the study area were selected and added to the model. SWAT simulation was the final step which includes running the model and reading SWAT output.

3.3.3. Sensitivity analysis, calibration, and validation of the model

I. Sensitivity analysis

SWAT input parameters are process-based and must be held within a realistic uncertainty range. The first step in the calibration and validation process in SWAT is the determination of the most sensitive parameters for a given watershed. The user determines which variables to adjust in calibration based on the result from sensitivity analysis. Therefore, It's necessary to identify key parameters and the parameter precision required for calibration (Ma et al., 2000). Sixteen parameters that are sensitive to streamflow were chosen to do the sensitivity analysis. The selection of sensitive parameters was done by reviewing different literatures in Ethiopia Wakjira et al., 2016; Tadele 2007; Webster 2010). Parameters used for sensitivity analysis were described in Table 3-7.

Table 3-7. Selected parameters to do sensitive parameters.

No.	Parameter identifiers	Full name of the parameter
1	R__GW_REVAP.gw	Groundwater "revap" coefficient.
2	R__CANMX.hru	Maximum canopy storage.
3	R__HRU_SLP.hru	Average slope steepness
4	R__SOL_AWC(..).sol	Available water capacity of the soil layer.
5	R__REVAPMN.gw	Threshold depth of water in the shallow aquifer for "revap" to occur (mm).
6	R__SLSUBBSN.hru	Average slope length.
7	V__GWQMN.gw	Threshold depth of water in the shallow aquifer required for return flow to occur (mm)
8	R__CH_K2.rte	Effective hydraulic conductivity in main channel alluvium.
9	V__ALPHA_BF.gw	Baseflow alpha-factor (days).
10	R__OV_N.hru	Manning's "n" value for overland flow.
11	R__CH_N2.rte	Manning's "n" value for the main channel.
12	R__RCHRG_DP.gw	Deep aquifer percolation fraction.
13	V__GW_DELAY.gw	Groundwater delay (days).
14	R__ESCO.hru	Soil evaporation compensation factor.
15	R__SOL_BD(..).sol	Moist bulk density.
16	R__CN2.mgt	SCS runoff curve number

In this research, SUFI2 was used to identify the sensitive parameters. The global sensitivity analysis method was used in SUFI2 before calibration and the result was examined for this research. Global sensitivity analysis sees all variables' sensitivity at once but it needs a large number of simulations. In the global sensitivity parameter, t-stat and p-value are used to

identify the relative significance of each parameter. Larger t-stat in absolute value and p-value close to zero are more sensitive as suggested by the SUFI2 user manual.

In the sensitivity analysis process, the SWAT simulated "TxtInout" was copied to the working directory, and SWAT-CUP SUFI2 was used for performing the sensitivity of selected parameters with default upper and lower parameter bounds. The 16 flow parameters shown in Table 3-7, which are sensitive for streamflow were included for the sensitivity analysis. Upon completion of sensitivity analysis, a t-stat and p-value were used to identify the relative significance of each parameter.

II. Calibration

After sensitivity analysis, the most sensitive parameters were used for model calibration. Calibration was done to better parametrize a SWAT model to a given set of local circumstances, thereby reducing prediction uncertainty. Yenealem (2018) recommended that a combination of manual and auto-calibration help to do a good calibration. For this study, the first manual calibration was done and some parameters were adjusted in the SWAT model. Then auto-calibration was applied for the calibration of the SWAT model. In the SWAT-CUP calibration procedure, the SWAT 500 simulation was specified for performing the calibration as suggested by the SWAT cup user manual. Then, the desired parameters for optimization observed data, and methods of calibration were selected. Two-third of the total data (1989 to 2001) was used for calibration.

III. Validation

Validation was used to test the calibrated parameters with an independent set of data without further changes to parameters. For validation, one-third (2002-2006) of the total data was used. Both calibration and validation were done based on monthly streamflow data.

3.3.3.1. Model performance evaluation

To evaluate the model simulation outputs relative to the observed data, model performance evaluation is necessary. There is a various method to evaluate the model performance during calibration and validation periods. For this study coefficient of determination (R^2), Nash and Sutcliff simulation efficiency (NSE), and PBIAS were used.

The determination Coefficient describes the linear relationship between simulated and observed data. Its value ranges from zero to one. A higher value close to 1 indicates good co-relation and typically values greater than 0.6 are considered acceptable (Santhi et al., 2001).

$$R2 = \frac{[\sum(Qo - mean.Qo)(Qs - mean.Qs)]2}{\sum(Qo - mean.Qo)2 \ \sum(Qs - mean.Qs)2} \ldots\ldots\ldots\ldots\ldots (3.11)$$

The Nash and Sutcliffe simulation efficiency indicates how well the plots of observed versus simulated data fit the 1:1 line. The value ranges from negative infinity to one. Values greater than 0.5, indicate the simulated value predicted better. A value greater than 0.5 is acceptable performance (Santhi et al., 2001).

$$NSE = 1 - [\frac{\sum(Qo - Qs)2}{\sum(Qo - Mean.Qo)2}] \ldots\ldots\ldots\ldots\ldots\ldots\ldots\ldots (3.12)$$

The proportion of PBIAS describes the tendency of the simulated data to be greater or smaller than the observed data, expressed as a percentage. The optimum PBIAS value is zero and low indicates that the model simulation is satisfactory. Positive values indicate a tendency of the model to underestimate while negative values indicate overestimation (Moriasi, 2007).

$$PBIAS = [\frac{\sum(Qo - Qs)}{\sum Qo}] \ldots\ldots\ldots\ldots\ldots\ldots\ldots\ldots\ldots 3.13$$

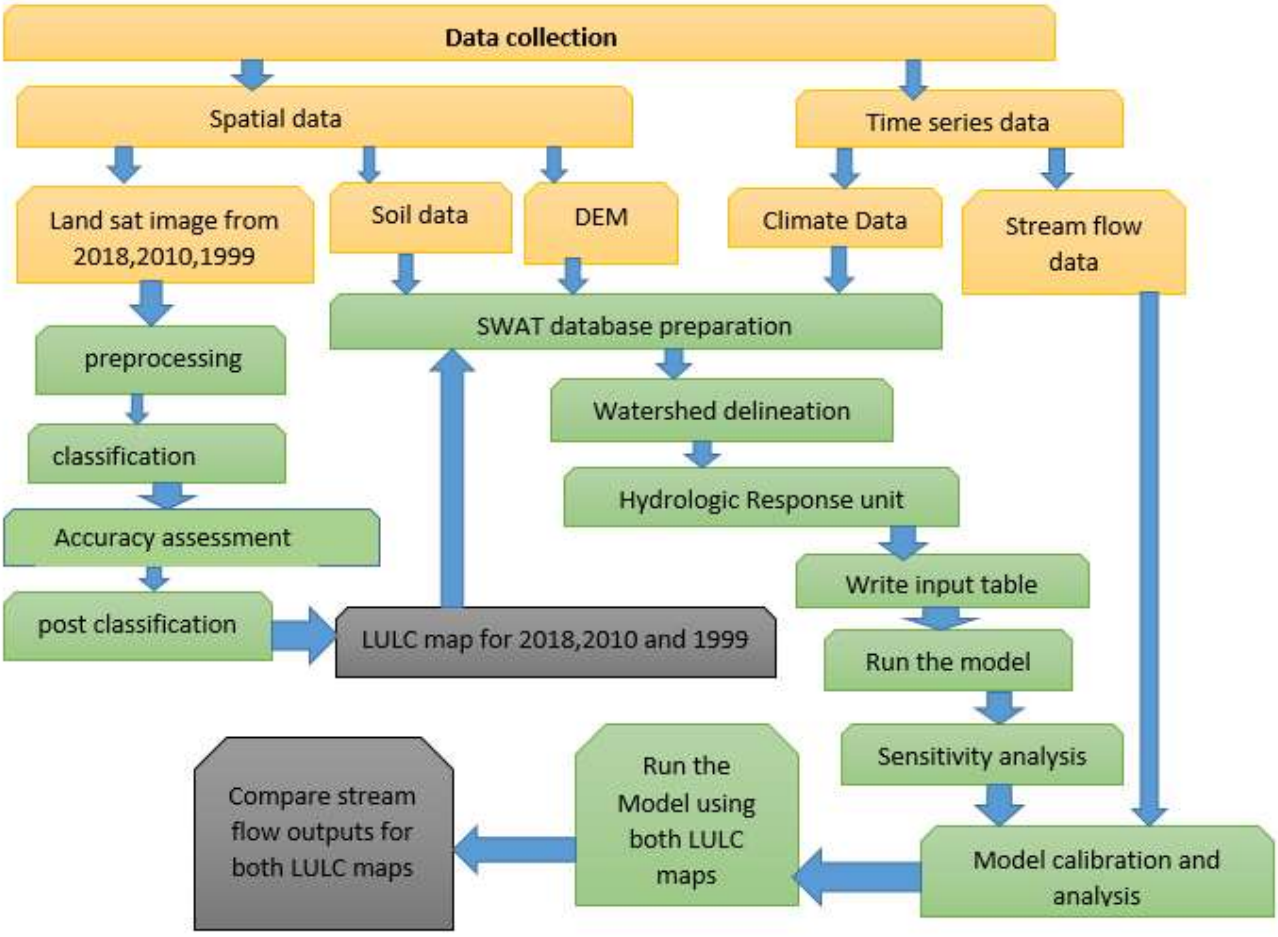

Figure 3-10. Framework of the study.

4. RESULT AND DISCUSSION

4.1.LULCC analysis

4.1.1. LULC change analysis

The major LULC types identified in the Deme catchment were Agricultural land, Grassland, Bushland, Forest, and Built-up areas. The classified maps for 1999, 2010, and 2018 as shown in Figure 4-1.

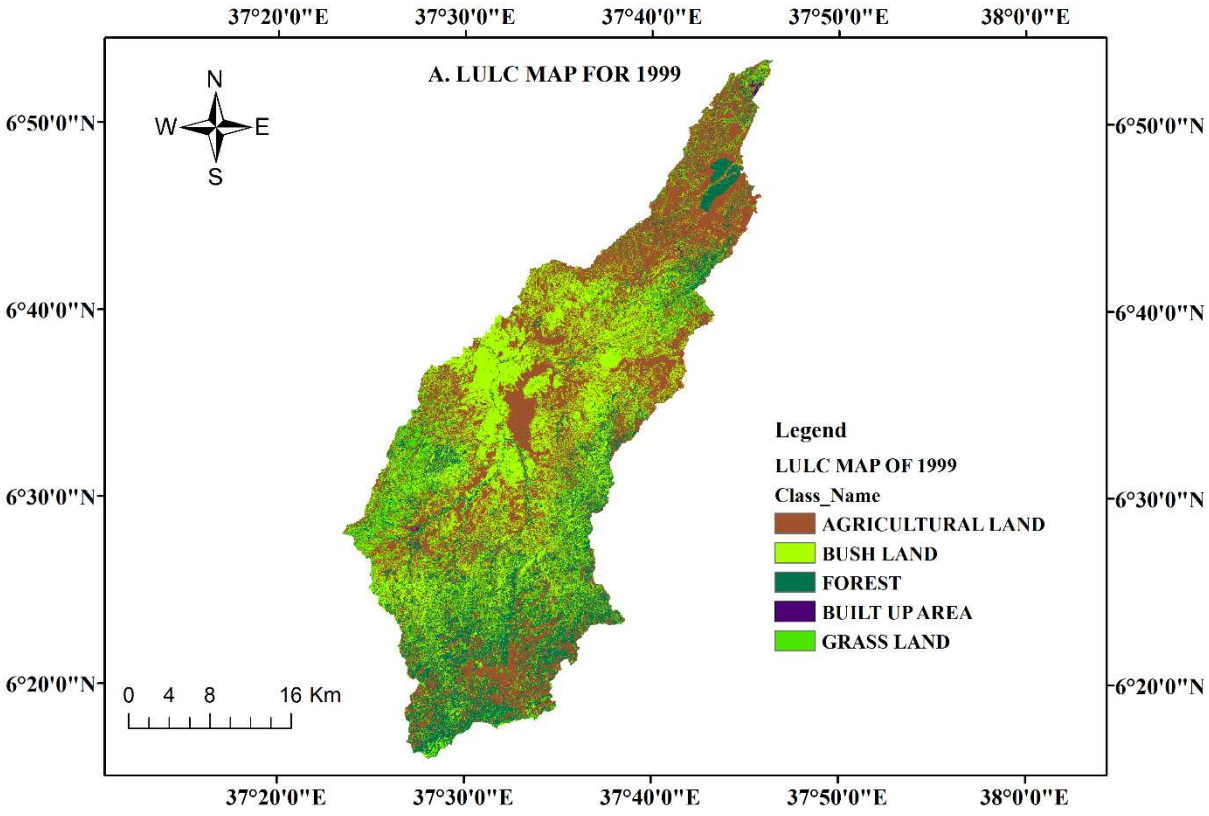

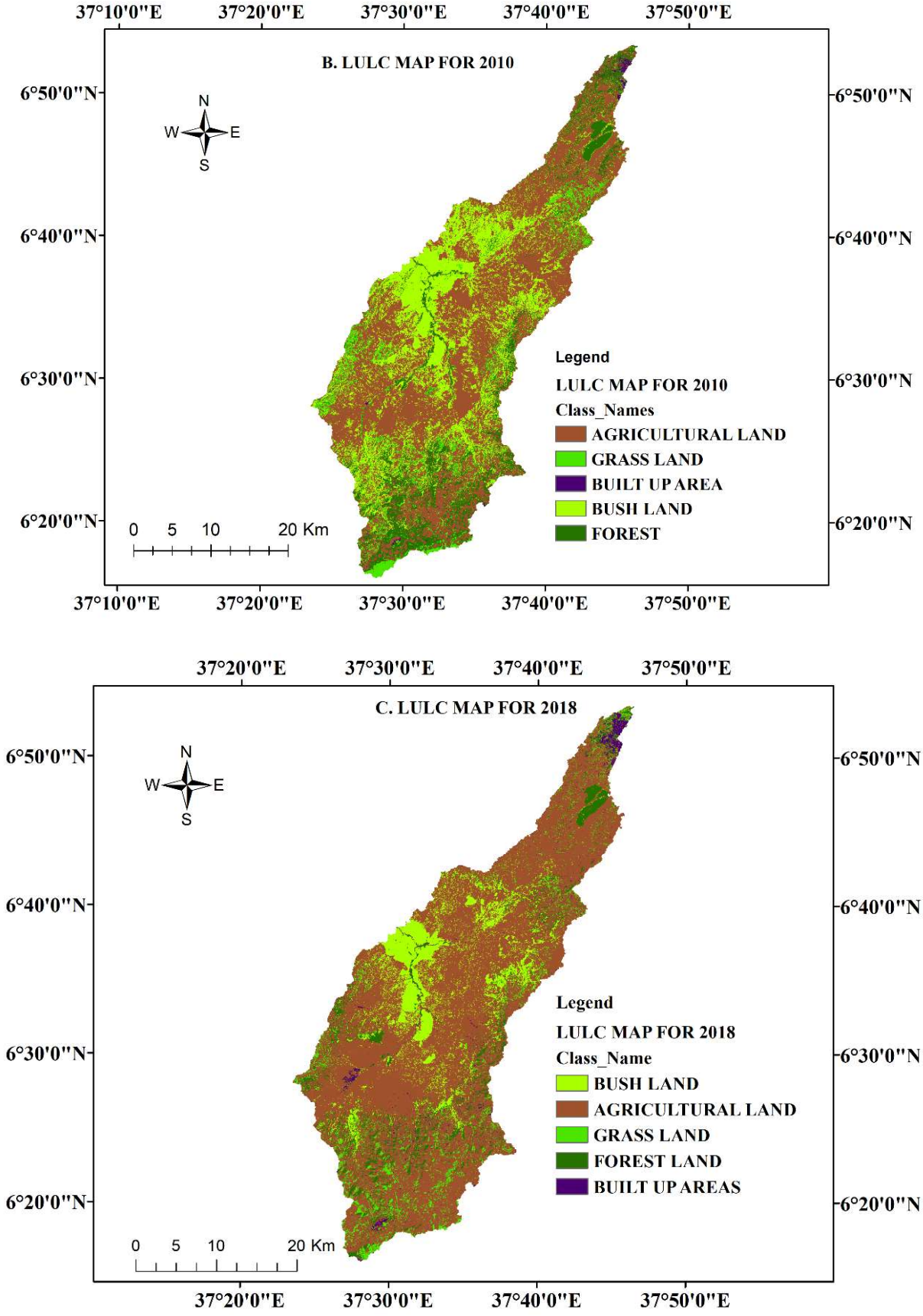

Figure 4 1. LULC map of A) 1999, B) 2010, and C) 2018.

The LULCC analysis showed that the occurrence of LULCC in the Deme catchment. The result was shown in the percent of temporal change and rate of change in Table 4-1.

Table 4-1. Area of LULC, temporal changes, and rate of change

LULC classes		AGRL	BSL	FRST	GRL	BTUA
Area in Km^2	1999	462.42	330.79	208.30	106.42	3.79
	2010	600.98	285.56	134.49	83.36	6.84
	2018	821.99	129.8	75.24	67.69	16.99
Area in percent	1999	41.60	29.75	18.74	9.57	0.34
	2010	54.06	25.69	12.10	7.54	0.62
	2018	73.94	11.68	6.77	6.09	1.53
Temporal change (%)	1999-2010	29.96	-13.67	-35.44	-21.20	80.41
	2010-2018	36.78	-54.55	-44.05	-19.28	148.47
	1999-2018	77.76	-60.76	-63.88	-36.39	348.27
Rate of Change (% /year	1999-2010	2.72	-1.24	-3.22	-1.93	7.31
	2010-2018	4.6	-6.82	-5.51	-2.41	18.56
	1999-2018	4.09	-3.20	-3.36	-1.92	18.33

The major LULCC trend observed includes a decline in Bush Land, Forest and Grassland, and expansion of agricultural land and built-up areas. Agricultural land which has always comprised the largest portion of the watershed area increased considerably between 1999 and 2018. During this period Agricultural land and the built-up area has increased by 77.76percent and by 348.27percent respectively.

In 1999, 41.60 percent of the watershed area was under agricultural land and in 2010 these values increased to 54.06 percent followed by a raise to 73.94 percent in 2018. This shows that the average changing rate to agricultural land is about 2.72percent per year in the year between 1999 and 2010. The agricultural land area in 2018 was raised to 821.99 Km^2 by the Changing rate of 4.6% per year. The built-up area was also another Class that increased its areal coverage during the study period. The built-up area was increased by 80.41 percent from 1999 to 2010

and by 148.47 percent (i.e. 1.5 folds from its previous area) from 2010 to 2018. Expansion of built-up area was very high in the northern tip of the watershed as clearly shown in Figure 4.1. Part of this area was the capital city of Wolaita administrative zone.

In the contrast, other classes such as Bushland, forest, and grassland are LULC classes which are progressively decreased during the study period. Bushland was reduced by 13.67 percent from 1999 to 2010 and by 54.55 percent from 2010 to 2018. Forest coverage decreased by 35.44 percent between 1999 and 2010 and by 44.05 percent between 2010 and 2018. Grassland decreased by 21.20 percent from 1999 to 2010 and by 19.28 percent from 2010 to 2018. The decrement of natural vegetation can be associated with the continuous increment of Agricultural area. Agricultural land demand increased due to population pressure. For instance, Selamber woreda (Kucha woreda), one of the towns constructed in the Deme catchment was densely populated from the Gamo zone, with 123 persons per square kilometer (Sintayehu 2016: Fikru 2012). According to Kucha woreda agricultural and rural development, the population in this woreda was 102,598, 149,835, and 179,498 in 1987,2007, and 2012 respectively. Agriculture is the main activity of the people living in Kucha woreda. Therefore, this population pressure and agricultural land demand lead to deforestation.

Studies in different parts of Ethiopia and around the Deme catchment came up with similar results. For example, in the Hare watershed, which is near to the Deme catchment LULCC analysis showed that the expansion of farmland and settlement from 1967-2004 (Tadele 2009). Another study Baso-Deme watershed revealed that LULC detection analysis over thirty years (1985-2014) depicts that there was a substantial alteration of cover types. The author reported that cropland showed a significant positive change by 46.8% (Teshome 2016). Similarly, another study in the Gojeb catchment showed that the catchment has undergone significant LULC changes. The major changes were the expansion of cropland at the expense of other

LULC classes at the rate of 29.56% in 1978, 38.91% in 1987, 46.62% in 2001, and 52.74% in 2015 (Melku et al., 2020).

4.1.2. Accuracy assessment

The final step in LULC classification was accuracy assessment. It tells us how effectively the pixels were sampled correctly to respective LULC classes. ERDAS IMAGINE was used to perform a method of confusion matrix to assess classification accuracy. The overall classification accuracy which is the ratio of the total number of correctly classified pixels to the total number of reference pixels was shown to be 86.6%, 90.93%, and 92.49% respectively for 1999, 2010, and 2018 LULC map. This showed that the classification was accurate enough to use.

Table 4-2. Confusion matrix for LULC map of 1999.

Classified data for 1999	Reference data for 1999						Accuracy	
	AGRL	BSL	FRST	BTUA	GRL	Row total	producers	users
AGRL	88	11	0	0	0	99	88	89
BSL	0	96	11	0	13	120	90	80
FRST	12	0	100	4	1	117	90	85
BTUA	0	0	0	6	0	6	60	100
GRL	0	0	0	0	44	44	76	100
Column total	100	107	111	10	58	386		

Legend: AGRL=agricultural land, BSL=bush land FRST= forest, GRL=grass land BTUA= built-up area.

Table 4-3. Confusion matrix for LULC map of 2010.

Classified data for 1999	Reference data for 2010						Accuracy	
	AGRL	GRL	BTUA	BSL	FRST	Row total	producers	Users
AGRL	117	5	0	0	9	131	94	89
GRL	0	25	5	0	0	30	64	83
BTUA	0	0	17	0	0	17	77	100
BSL	7	8	0	89	0	104	100	86
FRST	0	1	0	0	103	104	92	99
Column total	124	39	22	89	112	386		

Legend: AGRL=agricultural land, BSL=bush land FRST= forest, GRL=grass land BTUA= built up area.

Table 4-4. Confusion matrix for LULC map of 2018.

Classified data for 1999	Reference data for 2018						Accuracy	
	BSL	AGRL	GRL	FRST	BUTA	Row total	producers	users
BSL	87	0	0	0	0	87	100	100
AGRL	0	141	19	9	0	169	100	83
GRL	0	0	25	1	1	26	57	96
FRST	0	0	0	68	0	68	87	100
BTUA	0	0	0	0	36	36	100	100
Column total	87	141	44	78	36	386		

Legend: AGRL=agricultural land, BSL=bush land FRST= forest, GRL=grass land BTUA= built up area.

4.2. SWAT model sensitivity analysis, calibration, and validation

I. Sensitivity analysis

For global sensitivity analysis sixteen (16) flow parameters were considered which may affect streamflow. AS clearly shown in Appendix 4, the result of Global sensitivity analysis showed

that R_CN2.mgt, R_SOL_BD.sol, R_ESCO.hru, and V_GW_DELY.gw were the most sensitive parameter with P-value 0.00, 0.00, 0.05, and 0.08 respectively. These sensitive parameters were used during model calibration. The P-value and t-value were shown in appendix 3. The higher t-stat and the lower p-value indicate that the parameter was sensitive as suggested by the SWAT CUP manual user.

II. Calibration

The monthly flow of the Deme catchment from 1989 to 2001 was used for calibration. The first two years from the recorded data, 1989 and 1990, were used as a model "warm-up" Period to establish proper initial conditions and stabilize the model as suggested by SWAT manual users. Sensitive parameters were varied several times to obtain an acceptable value for R^2, NSE, and PBIAS. The calibration was done until the simulated flow closely matched the observed flow. The calibration result showed that the result of R^2, NSE, and PBIAS were 0.80, 0.75, and -1.2. This indicated that the model performance assessment indicated a good correlation and agreement between the monthly measured data and simulated flow. The figure also showed that the model performance was good. The figure also showed that the model performance was good.

Table 4-5. Sensitive parameters used during calibration

Parameter_Name	Fitted_Value	Min_value	Max_value
1:R__CN2.mgt	-0.6955	-0.80	0.80
3:V__GW_DELAY.gw	0.017329	-0.034891	0.034891
6:R__ESCO.hru	0.675333	0.5	0.9
12:R__SOL_BD(..).sol	-0.004336	-0.005061	0.005061

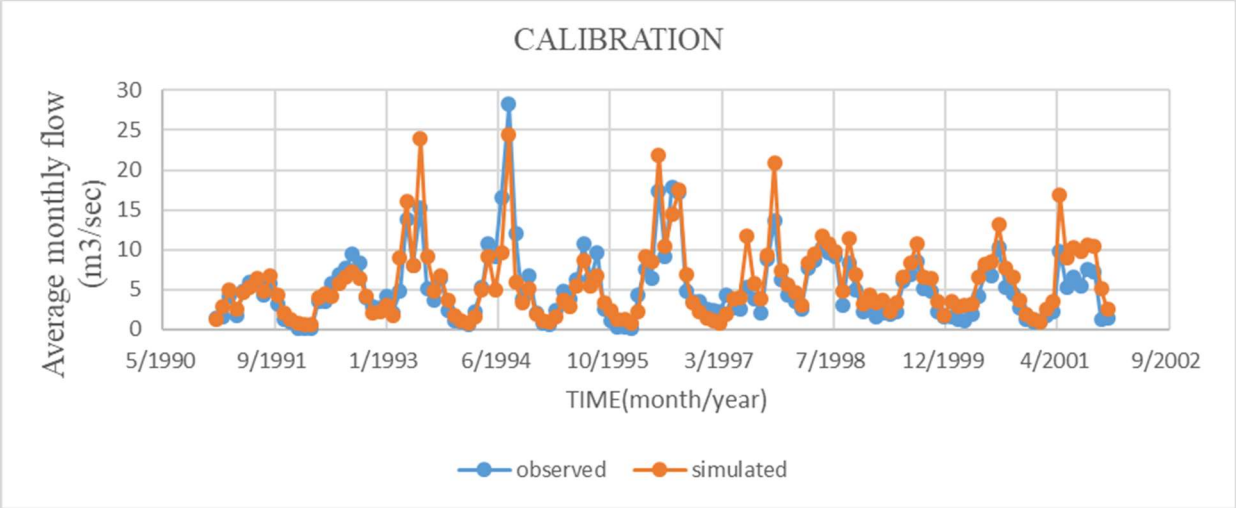

Figure 4-1. Stream flow hydrograph for the calibration on the monthly time step.

III. validation

Model validation was done from 2002 to 2006 monthly flow data. The result indicated that the model is capable of predicting the watershed streamflow in a good manner. During validation NSE and R^2 values were 0.70 and 0.74 for respectively. This agrees with the case study reported by Tadele 2009 in the Hare River watershed, which is near to the Deme catchment. Tadele 2009, reported that R^2 value was 0.72 to 0.85 and NSE from 0. 66 to 0.8 for monthly data. SWAT model was used with the calibrated value of 0.75, 0.65 and 12.7 for R^2, NSE, and PBIAS respecyively and validated value of 0.78, 0.65, and -22.6 for R^2, ENS, and PBIAS respectively in Upper Gidabo watershed to analyze the impact of LULCC on streamflow (Mamuye, 2020).

Table 4-6. Monthly time step calibration and validation statics

Time period	Evaluation criteria		
	R^2	ENS	PBIAS
Calibration (1991-2001)	0.80	0.75	-1.2
Validation (2002-2006)	0.74	0.70	-7.3

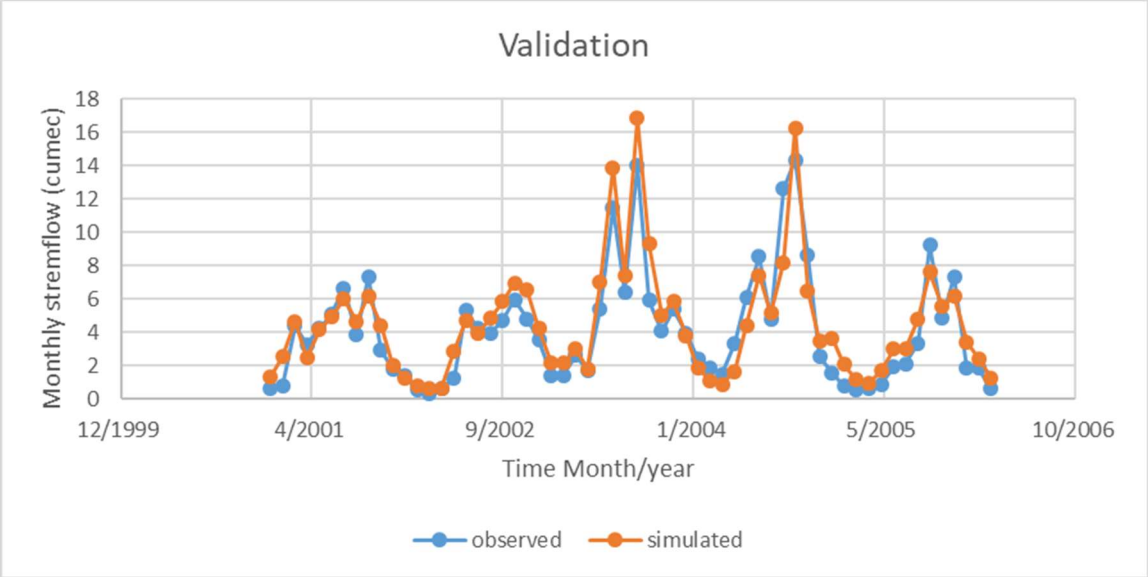

Figure 4-2. Stream flow hydrograph for validation on the monthly time step.

4.3. Impact of LULCC on streamflow of Deme catchment

One of the most important parts of the study was to evaluate the response of streamflow under different LULC in the Deme catchment. Surface run-off, lateral soil flow, and groundwater flow are the components of streamflow that were affected by LULCC, and the evaluation was done depending on this value at the outlet of the Deme catchment. The streamflow due to the three LULC maps was simulated and then compared to analyze the impact. The output of the simulated streamflow was grouped into four Ethiopian seasons (Bega, Tsedey, Kiremt, and Belg) to see the seasonal variability of streamflow.

The result in Tables 4-7 showed that streamflow decreased in the dry season (Bega) and increased in the wettest season (Kiremt). The streamflow decreased by -0.4m^3/sec and -0.76m^3/sec during the first and second periods in the dry season (Bega). During the wettest season (Kiremt) streamflow increased by 0.9m^3/sec and 2m^3/sec from 1999 to 2010 and 2010 to 2018 respectively. Generally, Streamflow increased in the wet season (Kiremt) and decreased in the dry season (Bega).

Table 4-7. Review on seasonal flow variability due to LULCC

Flow seasons	Simulated streamflow (m^3/sec)			Change in magnitude (m3/sec)		Change in percent (%)	
	1999	2010	2018	1999-2010	2010-2018	1999-2010	2010-2018
Bega (Winter)	2.41	2.01	1.25	-0.4	-0.76	-16.71	-37.81
Tsedey (Spring)	5.13	5.75	7.13	0.62	1.38	12.11	24.00
Kiremt (Summer	7.06	7.96	9.97	0.90	2.00	12.79	25.16
Belg (Autumn)	4.44	4.29	3.89	-0.15	-0.4	-3.38	-9.32

Note that Kiremt extends from Jun-August; Belg extends from September-November; Bega extends from December-February; Tsedey extends from March-May.

For assessing the change in seasonal variability of streamflow, the analysis was done on streamflow components SURQ, GWQ, and LATQ. Table 4-9 clearly show that the contribution of SURQ was less in the dry season than in the wet season. For instance, from 1999 to 2010, in the dry season the contribution of Surface runoff (SURQ) 0.22mm which is less than the contribution in the wettest season 1.7mm. Similarly, the lateral flow was showed a decrement through all seasons. The contribution from groundwater flow was also reduced by -1.08mm and by -2.13mm in both periods during the dry season (Bega). During the dry season streamflow was mainly comes from groundwater. So that, in dry season stream flow decreased.

Table 4-8. Seasonal variation of Surface runoff due to LULCC.

Year of simulation		SURQ(mm)	LATQ(mm)	GWQ(mm)
199	Bega (Winter)	3.36	2.08	17.78
	Tsedey (Spring)	19.27	6.09	51.71
	Kiremt (Summer)	31.27	9.96	92.81
	Belg (Autumn)	13.48	7.12	65.14
2010	Bega (Winter)	3.58	1.91	16.70
	Tsedey (Autumn)	20.44	5.58	46.62
	Kiremt (Summer)	32.97	9.1	85.19
	Belg (Autumn)	14.27	6.53	61.75
2018	Bega (Winter)	3.88	1.67	14.57
	Tsedey (Spring)	22.03	4.73	41.16
	Kiremt (Summer)	35.28	7.72	76.61
	Belg (Autumn)	15.39	5.67	56.61

Table 4-9. Seasonal variability of Surface runoff, lateral flow, and Groundwater flow

Seasons	Change in mm 1999-2010			Change in mm 2010-2018		
	SURQ	LATQ	GWQ	SURQ	LATQ	GWQ
Bega	0.22	-0.18	-1.08	0.3	-0.24	-2.13
Tsedey	1.17	-0.52	-5.09	1.58	-0.85	-5.46
Kiremt	1.7	-0.87	-7.63	2.31	-1.38	-8.57
Belg	0.79	-0.59	-3.39	1.12	-0.86	-5.14

The simulated annual streamflow value shows an increment from 1999 to 2010 and 2010 to 2018 respectively. This is due to the cumulative increment during the wet season (Kiremt) was higher than the dry season (Bega). Table 4-10, reviews the annual stream value and the change for the study period.

Table 4-10. Simulated mean annual streamflow and changes in the study period.

Year	1999	2010	2018	change in magnitude		Change by percent	
				1999-2010	2010-2018	1999-2010	2010-2018
Stream-flow (m^3/sec)	4.735	5.013	5.59	0.278	0.57	5.91%	11.37%

For assessing change in the contribution of annual streamflow, components due to LULCC, analyses were made on annual values of surface runoff (SURQ), Groundwater flow (GWQ), and Lateral flow (LATQ). As shown in Table 4-10 surface runoff has increased and the other components decreased in both periods.

Table 4-11. Annual variation in surface runoff, and lateral flow, and groundwater flow

Hydrologic components	1999	2010	2018	Change from 199-2010	Change from 2010-2018
SURQ(mm)	202.2	213.83	229.77	11.63	15.94
GW-shallow Aquifer (mm)	705.47	701.7	697.03	-3.77	-4.67
LATQ (mm)	75.81	69.34	59.38	-6.47	-9.96
Percolation	757.28	753.3	748.4	-3.98	-4.9
Total-Aqufer recharge	754.22	750.24	745.35	-3.98	-4.89

The increase of SURQ and decrease of LATQ and GWQ was due to the expansion of agricultural land and built-up area and as well as the decrement of Forest, Bush land and Grass land. When agricultural land is plowed, compaction of lower soil horizon occurs and this lowers infiltration rate and increases bulk density (Abu-Handeh, 2003). Runoff is dependent on antecedent soil water condition, which is a function of bulk density. Additionally, agricultural land demands less soil moisture than forest and generate runoff quickly than forest-covered area. Therefore, agricultural land gives immediate response to rainfall. Forest tends to decrease the generation of runoff; thus smaller area of forest has a greater tendency to generate more runoff (Teferi et al., 2010). Generally, as agricultural and built-up area increases, infiltration, percolation out of the soil to groundwater decreases thereby decreasing groundwater recharge and increasing surface runoff. This result demonstrates that LULCC has significant effects on infiltration rates, on water retention capacity of soils, on sub-surface transmissivity, and surface runoff production.

Different studies have been conducted in different parts of Ethiopia to evaluate the effects of LULCC on streamflow. In the study of Hydrologic response to LULCC in the upper Gidabo watershed Streamflow increased during the wet season by 5.6% and dry season decreased by 12.7% (Mamuye, et al 2020). Another study in the Hare watershed reported the increase of

streamflow in the wet season by 12.5% and decreased in the dry season by 30.5% (Tadele 2009). This study (Tadele, 2009), revealed that the increment of Surface runoff from 39% to 44%. On the other hand, decrement in groundwater flows from 49% to 42%. Additionally, the study Assessment of LULCC impact on streamflow of Katar catchment, confirmed that surface runoff increased by 48.46 from 1995 to 2015 and the groundwater flow decreased by 30.97% from 1995 to 2015 (Tolera, 2018).

Numerous studies have also shown that the increment of mean annual streamflow due to LULCC. For instance, the study under the title impact of LULCC on streamflow and sediment yield in Gidabo catchment revealed that the increment of mean annual streamflow by 29% (Shemeles, 2017). Tan et al. (2015) studied the impact of LULCC on the Johor river and revealed that the increment of Annual streamflow by 4.4% due to LULCC experienced in Johor catchment. The study reported that the increase in annual streamflow was due to the change of forest land to agricultural land. Generally, the result of the analysis indicated that LULCC has altered the streamflow and its components.

5. SUMMARY AND CONCLUSION

5.1.Summary

In this study, the SWAT model was used to evaluate the impacts of LULCC on the streamflow of the Deme catchment. To do this, satellite images were used to produce the map of different LULC classes. ERDAS IMAGIN2014 was used for classification and accuracy assessment of the map produced. The SWAT 2012 model was calibrated and validated in the Deme catchment and the performance of the model was seen. Then the Evaluation of LULCC on streamflow was done.

The LULCC analysis during the study period (1999-2018) indicated a significant change of LULC in the Deme catchment. The study showed that the expansion of agricultural land and built-up area, and the degradation of bushland, forest, and grassland. The decrement of natural vegetation was related to the expansion of agricultural land and the built-up area in the watershed during the study period. During 1999 agricultural land was covered 462.4Km^2 which is then increased by to 600.98Km^2 in 2010. Again agricultural land increased by 36.78% to 821.99Km^2 in 2018. The built-up area was also the other LULC class which increased throughout the study period Built-up area increased from 3.79Km^2 to 6.84Km^2 by 80.41% and increased to 16.99Km^2 in 2018 by 148.47%. The other LULC classes showed a decrement in all periods.

For hydrological modeling, a global sensitivity analysis using SWAT CUP (SUFI-2) sixteen flow parameters that may affect streamflow were considered from different works of literature. From those parameters three parameters CN2.mgt, SOL_BD.sol, ESCO.hru and GW_DELY.gw, were found to be most sensitive in the Deme catchment. The graphical and statistical results both during calibration and validation showed adequate model performance. During calibration, the value of R^2, NSE, and PBIAS was 0.80, 0.75 and -1.2 respectively. The validation value for R^2, NSE, and PBIAS was 0.74, 0.70 and -7.3 respectively. Performance

evaluation analysis of the model showed that the SWAT model can predict streamflow within an acceptable range of error.

The impact of LULCC on streamflow was done after effective calibration and validation of the model at the gauging location (Oratalem). The seasonal value of Deme catchment streamflow showed variability due to LULCC induced from 1999 to 2018. During the driest season (Bega), decreased by -16.71% from 2.41m^3/sec to 2.01m^3/sec from 1999 to 2010 and again decreased by -37.81% from 2.01m^3/sec to 1.25m^3/sec from 2010 to 2018. In contrast during the wettest season (Kiremt) Streamflow increased by 12.79% from 7.06m^3/sec to 7.96m^3/sec from 1999 to 2010 and increased again by 25.16% from 7.96m3/sec to 9.97m^3/sec from 2010 to 2018. This is directly attributed to the expansion of agricultural land over natural vegetation (Forest, grassland, and bushland) that results in the increase of surface runoff following rainfall events and causes variation in soil moisture condition and groundwater storage. This expansion also results in the reduction of water infiltrating into the ground and supplying the shallow aquifer. Therefore, the flow during the dry season (which mostly comes from base flow) decreases whereas the flow during the wet season increases.

The contribution of surface runoff, lateral flow, and the groundwater flow to the Deme catchment streamflow due to LULCC indicated a variation with change in LULC. Surface runoff increased by 11.63mm from 1999-2010 and 15.49mm from 2010-2018. Shallow groundwater recharge decreased by 3.77mm from 1999-2010 and 4.67mm from 2010-2018. Similarly, lateral flow decreased by 6.47mm from 199-2010 and 9.96mm from 2010-2018. The increment and decrement value in the second phase exceeds the first phase. This was directly attributed to the expansion of agricultural land and built-up area, which was higher in the second phase.

5.2.Conclusion

This study aimed to evaluate the impact of LULCC on the Deme catchment from 1989 to 2018. From this study, it can be concluded that the Deme catchment had experienced a significant change in LULC. It is identified that LULCCs have a similar trend during the two periods (1989-2010 and 2010-2018). Part of the Forest, grassland, and bushland was changed into the built-up area and built-up areas. However, the predominant change in LULC during the whole period is the increase in agricultural land and the overall decline in the forest, grassland, and bushland.

The SWAT model was employed to predict the impact of LULCC on the streamflow of the Deme catchment. The hydrologic components of the SWAT model were calibrated and validated after sensitivity analysis. The sensitivity analysis has pointed out the three most sensitive parameters that control the surface and sub-surface hydrological process of the Deme catchment. These sensitive parameters were R_CN2.mgt, R_SOL_BD.sol, and R_ESCO.hru. on the other hand, calibration and validation values have shown that the predicted values have agreed well with the observed data at the outlet of the Deme catchment. Therefore, the SWAT model is capable to estimate streamflow composition and contribution from different LULC classes.

The impact of LULCC on streamflow was also investigated in this study. The result showed that streamflow in the dry season decreased and increased in the wet season for all LULC scenarios. Under the current set of model parameters, the result of the simulation demonstrated that the decrease in stream flow during dry(Bega) season flow that has direct relation to the water demand during this period. The increase of streamflow in wet season could causes flooding in the area. These changes in streamflow were particularly due to the change of natural vegetation (i.e. forest, bushland and grassland) to agricultural land and built-up area.

The evaluation of LULCC on streamflow visualized reasonably for the possible changes that affect the availability of streamflow, surface runoff, groundwater flow, and lateral flow. Generally, the following recommendations were given based on the analysis of LULCC impacts on hydrologic components of Deme catchment.

- ✓ In this regard, quantifying and addressing the fate sustainability of the water resource is importantly needed by planners and managers to work on the policy issue concerning spatial planning of land and water in use in the watershed.
- ✓ It is mandatory to restore the degraded area of the watershed to minimize the negative impact of LULCC like flooding, and the decrease of streamflow in dry season.
- ✓ Another study should be done like, the impact of Climate change on hydrology of Deme catchment.

6. REFERENCE

Abebe, S. (2005). Land-Use and Land-Cover Change in Head Stream of Abbay Watershed, Blue Nile Basin, Ethiopia. Addis Ababa University.

Abu-Handeh, N.H. (2003). Compaction and Subsoiling Effects On Corn Growth and Soil Bulk density. Soil Sci. Soc. Am. J., Vol(67): Pp. 1213-1219.

Amanuel, A and Mulugeta, L (2014). Detecting and quantifying LULC dynamics in Nadda Asendabo watershed southwestern Ethiopia, journal of Environmental science, vol(3), Pp45-50.

Arnold, J. G., Allen. P. M. And Bernhardt. G. (1993). A Comprehensive Surface-Groundwater Flow Model. Journal of Hydrology, Vol(142): Pp 47-69.

Ashebir, W.Y., Marc, C., Girma, K. and Wubneshe, D. (2018). LULCCs and Their Effects On the Landscape of Abaya-Chamo Basin, Southern Ethiopia. Journal of land, Vol.7(1).

Asmamaw, A. (2013). Assessing The Impacts of Land Use and Land Cover Change On Hydrology of Watershed: A Case Study On Gilgel–Abbay Watershed, Lake Tana Basin, Ethiopia. Dissertation submitted in partial fulfillment for the degree of MSc. In geospatial technologies, Pp. 43-54

Assefa B (2012). Land use land cover change and its effect on existing forest condition, the case of Shakiso natural forest, southeast Ethiopia. Hawassa university, Wondo Genet college of forestry and Natural resources, Wondo Genet, Ethiopia.

Awulachew, S.B., Tenaw, M., Steenhuis, T., Easton, Z., Ahmed, A., Bashar, K.E., and Hailesellassie, A. (2008). Impact of Watershed Interventions On Runoff and Sedimentation in Gumera Watershed. Fighting poverty through sustainable:

proceedings of the CPWF Second international forum on water and food Addis Ababa Ethiopia. Vol.1.

Ayana, A.B., Edossa, D.C. and Kositsakulchai, E. (2014). Modeling The Effects of Land Use Changes and Management Practices On Runoff and Sediment Yields in Fincha Watershed, Blue Nile, OIDA. International Journal of Sustainable Development. Journal of Land. Vol.9(113). Doi 10.3390/land9040113.

Benito, G., Rico, M., Sanchez-Moya, Y., Sopeña, A., Thorndycraft, V.R. and Barriendos, M. (2010). The Impact of Late Holocene Climatic Variability and Land Use Change On the Flood Hydrology of the Guadalentin River, Southeast Spain. Global and planetary change. Vol.70(1). Pp. 53-63.

Bezawit A. (2011). Discharge and Sediment Yield Modeling in Enkulal Watershed, Lake Tana Region, Ethiopia. Thesis. Faculty of the Graduate school of Cornell University.

Bicknell, B.R., Imhoff, J.C., Kittle, J.L., Donigian, A.S. and Johanson, R.C. (2001). Hydrologic Simulation Program-FORTRAN. User 'S Manual, Athens, GA., USEPA. Vol(1).

Bireda, A. (2015). GIS and Remote Sensing Based Land Use/Land Cover Change Detection and Prediction in Fagita Lekoma Woreda, Awi Zone, North Western Ethiopia, Addis Ababa University School of Graduate Studies, MSc Thesis, Department of Geography and Environmental Studies.

Burch, G.J., Bath, R.K., Moore, I.D. and O'Loughlin, E.M. (1987). A Comparative Hydrological Behavior of Forested and Cleared Catchments in South Eastern Australia. Journal of Hydrology, Vol(90): Pp.19-42

Caetano, M., Mata, F., Freire, S. (2005). Accuracy Assessment of the Portuguese CORINE Land Cover Map. Global Developments in environmental earth observation from space. Proceeding of the 25th EARSeL Symposium, Porto, Portugal, Pp. 459-467.

Caldera, H.P.G.M., Piyathisse, V.R.P.C. and Nandalal, K.D.W., (2016). A Comparison of Methods of Estimating Missing Daily Rainfall Data, The Institution of Engineers, Sri Lanka, ENGINEER, Pp.1-8.

Cibin, R., Sudhee, R K. P. and Chaubey, I. (2010). Sensitivity and Identify Ability of Stream Flow Generation Parameters of The SWAT Model. Department of Agricultural and Biological Engineering, Purdue University, USA. Journal Hydrological process. Vol(24): Pp.1133-1148.

Cochran, W.G (1977). Sampling techniques. Third Edition. New York: John Willey and Son.

Costa, M.H., Botta, A. and Cardille, J.A. (2003). Effects of Large-Scale Changes in Land Cover On the Discharge of the Tocantins River, Amazonia. Journal of Hydrology, Vol(283), Pp. 206-217.

Cunderlik, J. (2003). Hydrological Model Selection for CFCAS Project, Assessment of Water Resource Risk and Vulnerability to Change in Climate Condition, University of Western Ontario. Journal of Environmental science. Corpus id:54992658.

Data D. (2006). Enduring Issues in State-Society Relations in Ethiopia: A Case Study of the WoGaGoDa Conflict in Wolaita, Southern Ethiopia. International Journal of Ethiopian Studies, Vol. 2, pp. 141-159.

De Silva, R. P., Dayawansa, N. D. K. and Ratnasiri, M. D. (2007). A Comparison of Methods Used in Estimating Missing Rainfall Data. Journal of Agricultural Sciences, Vol(3): Pp.101–108.

Deer, P.J., (1995). Digital Change Detection Techniques Civilian and Military Applications International Symposium On Spectral Sensing Research Report. Greenbelt MD. Goddard space flight center.

Devereux, S (2000). Food insecurity in Ethiopia. A discussion paper for DFID. Institute of development studies, Sussex.

Di Gregorio, A., and Jansen, L.J. (2000). Land-Cover Classification: Classification Concepts and User Manual, Food and Agriculture Organization (FAO) Of The United Nations Rome. Environmental and natural resources service, GCP/RAF/287/ITA Africover-. East Africa project and soil resources, Management, and conservation services.

Elnazier, R., Xue-Zhi, F. and Zheng, C. (2004). Satellite Remote Sensing for Urban Growth Assessment in Shaoxing City, Zhejang Province, Journal of Zhejiang University Science Vol.5(9).

Feddema, J. J., Oleson, K.W., Bonan, G.B., Mearns, L.O., Buja, L.E. and Meehl, G.A. (2005). Washington, W.M.: The Importance of Land-Cover Change in Simulating Future Climates. Journal of Science. Vol.310(5754): Pp. 1674-1678.

Fekadu Bekele, Ethiopian National Metrological Services Agency, http://ccb.colorado.edu/ijas/ijasno2/bekele.html, Addis Ababa, Ethiopia.

Fikru, H.A. (2012). The role of butter production and marketing in the livelihood of rural communities in Kucha woreda of Gamo Gofa Zone SNNPR. A thesis submitted to the center for rural development studies, Addis Ababa University, Addis Ababa, Ethiopia. Pp.26.

Food and Agricultural Organization (FAO) (2005). Global forest resources assessment. Progress towards sustainable forest management. FAO forestry paper 147, Rome.

Foody, G.M. (2002). "Status of Land Cover Classification Accuracy Assessment", Remote Sensing of Environment, Vol(80)): Pp. 185-201

Fu, B., Chen, L., Ma, K., Zhou, H. and Wang, J. (2000). The Relationships Between Land Use and Soil Conditions in The Hilly Area of the Loess Plateau in Northern Shaanxi, China. CATENA Vol. 39(1): Pp. 69-79.

Gan, T.Y. (1988). Application of Scientific Modeling of Hydrologic Response from Hypothetical Small Catchments to Assess a Complex Conceptual Rainfall-Runoff Model. Water Resources Series Technical Support No.111 University of Washington, Seattle, Washington.

Gayathri, K.D., Ganasri, B.P. and Dwarakish, G.S. (2015). Review On Hydrologic Models. International Conference On Water Resources, Coastal and Ocean Engineering. Peer-Review Under Under Responsibility of Organizing Committee of ICWRCOE.

Gebrehiwet, K. B. (2004). Land Use and Land Cover Changes in The Central Highlands of Ethiopia: The Case of Yerer Mountain and Its Surroundings. M.Sc Thesis, Addis Ababa University, Environmental Science.

Gereta, E. J., Chiombola, E.A.T., And Wolanski, E. (2001). Assessment of The Environmental Social and Economic Impacts On the Serengeti Ecosystem of the Development in the Mara River Catchments. Zoologische Gesellschaft, Frunkfurt Zoological society. Tanzania National Parks, Pp.46-49.

Getachew, H.E. And Melesse, A. (2012). The Impact of Land Use Change On the Hydrology of The Angereb Watershed, Ethiopia. International Journal of Water Sciences, Vol. 1(4).

Gordon, L. J., Steffen, W., Jönsson, B. F., Folke, C., Falkenmark, M., And Johannessen, Å. (2005). Human Modification of Global Water Vapor Flows from The Land Surface, P. Natl. Acad. Sci. USA, Vol(102): Pp. 7612–7617.

Green W.H. And Ampt G.A., (1911). Studies On Soil Physics,1. The Flow of Air and Water Through Soils. Journal of Agricultural Sciences, Vol(4): Pp 11-24.

Guo, H., Hu, Q. and Jiang, T. (2008). Annual and Seasonal Stream Flow Responses to Climate and Land-Cover Changes in The Poyang Lake Basin, China. Journal of Hydrology, Vol(355): Pp. 106-122.

Hadgu, K. M. (2008). Temporal and Spatial Changes in Land Use Patterns and Biodiversity in Relation to Farm Productivity at Multiple Scales in Tigray, Ethiopia. PhD. Thesis Wageningen University, Wageningen, The Netherlands.

Hao, C., Luuk, F., Janteine, B., Fei. W., Simon, M., and Coen. R., (2019). Impact of LULCC and Climate Effects On Stream Flow in Chinese Loes Plateau: A Meta-Analysis. Science total environment. Doi 10.1016/ j.scitotenv.2019.134989.

Jensen, R., Gatrell, J., And Melean, D., (2005). Geo-Spatial Technology in Urban Environment. Springer-Verlag Berlin Heiderberg, Germany, Pp.47-54.

Jiang, S., Ren, L., Yomg, B., Singh, V.P., Yang, X., and Yuan, F. (2011). Quantifying the effects of climate variability and human activities on runoff from the Laohahe basin in northern China using three different methods. Hydrological Process. Doi: 10.1002/hyp/.8002.

Kassa, G. (2003). GIS-Based Analysis of Land Use and Land Cover, Land Degradation and Population Changes: A Study of Boru Metro Area of South Wello, Amhara Region, MA Thesis, Department of Geography, Addis Ababa University.

Khorram, S., Nelson, S., Cakir, H, And V. D. and Wiele, C. (2013). Digital Image Processing: Post-Processing and Data Integration, Principles of Applied remote sensing, Springer Science Business Media New York, Pp.83-114.

Kidane, W. And Bogale, G. (2017). Effect of Land Use Land Cover Dynamics On Hydrological Response of Watershed: Case Study of Tekeze Dam Watershed, Northern Ethiopia. International Soil and Water Conservation Research, Vol(5): Pp 1-16.

Kirby, J., Mainuddin, M., Ahmed, M.D., Palash, W., Quadir, M.E., Shah-Newaz, S.M. and Hossain, M.M. (2016). The Impact of Climate Change On Regional Water Balances in Bangladesh. Journal of hydrology regional studies, Vol(3): Pp. 285-311.

Lambin EF and Geist HJ (2003). Global Land use land cover change: what we have learned so far? Global change newsletter (46): 27-30.

Lambin, E. F., Samuel, B. and Geist, H. J. (2002). Global Land-Use and Land- Cover Change: What Have We Learned So Far? Global Change Newsletter, Land Use /Cover Change, Vol(82): Pp.321-331.

Lambin, E.F., Geist, H.J., and Lepers. E. (2003). Dynamics of Land Use and Land Cover Change in Tropical Regions. Annu. Rev. Environ. Resource,Vol(28): Pp.205-241.

Leh M, Bajwa S, Chaubey I (2011). Impact of Land use change on erosion risk: an integrated remote sensing, geographic information system, and modelling methodology. Department of Biological and Agricultural Engineering, University of Arkansas, Fayetteville, AR, USA.

Lillesand, T.M., Kiefer, R. and Chipman, J.W. (2004). Remote Sensing and Image Interpretation, 5th Edition. Inc. New York.

Lu, D. And Weng, Q. (2007). A Survey of Image Classification Methods and Techniques for Improving Classification Performance. International Journal of Remote Sensing, Vol. 28(5): Pp. 823-870).

Lu, D., Mausel, P., Brondizio, E., and Moran, E. (2004). Change Detection Techniques. International Journal of Remote Sensing.

Lunetta, R.S. And Elvidge, C.D.E. (1999). Application of Project Formulation and Analytical Approach, Remote Sensing Change Detection Environmental Monitoring Methods and Applications, Lendon: Taylor and Francis, Pp. 1-20.

Mamuye, B., Sirak, T., Brook, A., and Woldeamlak, B. (2020). Hydrologic Response to Land Use Land Cover in The Upper Gidabo Watershed. Journal of Hydro research, Vol(3): Pp.85-94.

Manandhar, R., Odeh, I. And Ancev, T. (2009). Improving The Accuracy of Land Use and Land Cover Classification of Landsat Data Using Post-Classification Enhancement. Journal of Remote sensing, Vol(1): Pp. 330-344.

Mango, L.M., Melesse, A.M., Mc Clain, M.E., Gann, D. and Stegn, S.G. (2010). Land Use and Climate Change Impacts On the Hydrology of the Upper Mara River Basin, Kenya; Results of Modeling Study to Support Better Resource Management.

Mao, D. and Cherkauer, K.A. (2009). Impacts of Land-Use Change On Hydrologic Responses in The Great Lakes Region. J HYDROL, Vol. 374(1-2): Pp. 71-82.

Mc Cornic, P.G., Kamara, A.B. and Girma, T. (2003). Integrated Water and Land Management Research and Capacity Building Priorities for Ethiopia, Proceeding of A MoWR/Earo/IWMI/ILRI International Workshop Held at ILRI, Addis Ababa,

Ethiopia 2-4 December 2002, IWMI, Colombo, Sri Lanka, And ILRI, Nairobi, Kenya, Pp. 267.

Melku, D., Asfaw K., Awdenegest, M., and Adane, A. (2020). LULCCs and Its Drivers in Gojeb Catchment, Omo Gibe Basin, Ethiopia. Journal of Agricultural and Environmental for International Development.

Meyer, W.B. And Turner, B. L. (1994). Changes in Land Use and Land Cover: A Global Perspective. Cambridge, Cambridge University Press. New York.

Milkias, I.G., Shukui, T. and Qing, Y. (2019). Urban land-use conflict in expansion areas of wolaita-Sodo town, SNNPR, Ethiopia. Journal of resource development and management. ISSN 2422-8397, Vol(52).

Mohan, S and Shrestha, M.N. (2000). A GIS-Based Integrated Model for Assessment of Hydrological Change Due to Land Use Modifications, Proceeding of Symposium On Restoration of Lakes and Wetlands, Indian Institute of Science, Banglore, India.

Moriasi N.D. (2007). Model Evaluation Guide Line for Systematic Quantification of Accuracy in Watershed Simulations. American Society of Agriculture and Biological Engineering.

Mtjaz, G., and Marina, P. (2012). Strengths, weaknesses, opportunities and threats of catchment modelling SWAT model. Journal of research gate. https://wwwreaserchgate.netpublication/221929439, Pp.59-62.

Mustard, J.F., And Fisher, T.R. (2004). Land Use and Hydrology. Horn Point Laboratory Center For the Environmental Science University of Maryland Cambridge.

Natkhin, M., Dietrich, O., Schafer M.P., and Lischeid, G. (2015). The Effect of Climate and Changing Land Use On Discharge Regime of Small Catchment in Tanzania. Reg. Environ Change, Vol(14): Pp.1269-1280.

Ndomba, P. (2002). SWAT Model Application in Data Scarce Tropical Complex Catchment in Tanzania.

Neitsch, S.L., Arnold, J.G., Kiniry, J.R. And Williams, J.R. (2005). Soil and Water Assessment Tool, Theoretical Documentation: Version 2005. Temple, TX. USDA Agricultural Research Service and Texas A & M Black Land Research Centre.

Oki, T., and Kanae, S. (2006). Global hydrological cycles and world water resources, science, vol(313), Pp1068-1072, doi:10.1126/science. 1128845.

Piao, S., Friedlingstein, P., Ciais, P., De Noblet-Ducoudré, N., Labat, D., and Zaehle, S. (2007). Changes in Climate and Land Use Have a Larger Direct Impact Than Rising CO2 On Global River Runoff Trends, P. Natl. Acad. Sci. USA, Vol(104): Pp. 15242–15247.

Qian, J., Zhou, Q., and Hou, Q. (2007). Comparison of Pixel-Based and Object-Oriented Classification Methods for Extracting Built-Up Areas in Arid zone. In ISPRS Workshop On Updating Geo-spatial Databases with Imagery & The 5th ISPRS Workshop On Dmgiss, Pp. 163–171.

Qiu, Y.Q., Jia, Y.W., Zhao, J.C., Wang, X., Bennett, J. and Zhou, Z. (2010). Valuation of Flood Reductions in The Yellow River Basin Under Land Use Change. J WATER RES PL-ASCE, Vol. 136(1): Pp. 106-115.

Remo, J. W. F., Pinter, N., and Heine, R. (2009). The Use of Retro- And Scenario-Modeling to Assess Effects of 100 Years' River of Engineering and Land-Cover Change On

Middle and Lower Mississippi River Flood Stages. J HYDROL, Vol. 376(3-4): Pp. 403-416.

Richard Woodroofe and Associate (1996). Omo-Gibe river basin integrated development of master plan study final report. Water resource survey and inventories, ministry of water resources, Addis Ababa, Vol(5).

Sage, C. (1994). Population and Income. In Meyer, W.B., and Turner, B. L. Change in Land Use and Land Cover. A Global Perspective Cambridge University Press: Cambridge, Pp. 263-285.

Sathian, K. And Symala, P. (2009). Application of GIS Integrated SWAT Model for Basin Level Water Balance, Indian J. Soil Cons.,Vol(37): Pp 100–105.

Setegn, S., Srinivasan, R., Dargahi, B. And Melesse, A. (2008). Spatial Delineation of Soil Erosion Vulnerability in The Lake Tana Basin, Ethiopia. The open Hydrology journal. The open hydrology Journal, Vol.2(1): Pp.49-62.

Shemeles. M. (2017). Impact of LULCC On Streamflow and Sediment Yield: Case Study On Gidabo River Catchment, Rift Valley Basin, Ethiopia. MSc. Thesis. Addis Ababa Science and Technology University.

Shimaa, M. (2015). Hydrological Modeling of the Simly Dam Watershed (Pakistan) Using GIS and SWAT model. Alexandria Engineering Journal, Vol(54): Pp 583–594.

Singh, A. (1989). Review Article Digital Change Detection Techniques Using Remotely-Sensed Data. International Journal of Remote Sensing, Vol(10): Pp. 989–1003.

Singh, V.P., and Woolhiser, D.A. (2002). Mathematical Modelling of Watershed Hydrology. J. Hydrol. Eng., Vol. 7(4): Pp. 270-292.

Sintayehu, M. (2016). Child Rural-Urban Migration and Migrant Sending Families Perception Towards Child Migration: The Case of Haleha Kebele, Kucha Woreda, Gamogofa Zone, SNNP, A Thesis Submitted to The School of Graduate Studies of Addis Ababa University.

Stehman, S.V. (2000). Practical implications of design-based sampling inference for thematic map accuracy assessment. Journal of Remote sensing of Environment, Vol(72): Pp. 35-45.

Stonestorm, D.A,Scanion, B.R, and Zhang, L (2009). Introduction to special section on impact of LULCC on water resources. Water Resource Research, Vol (45). W00A00, dio:10.1029/2009WR0079337.

Subramanya, K. (2008). Engineering Hydrology Book, Third Edition, Former Professor of Civil Engineering Indian Institute of Technology Kanpur, Tata Mcgraw-Hill Publishing Company, Pp 29-51.

Surur, A. (2010). Simulated Impact of Land Use Dynamics On Hydrology During A 20-65 Year Period of Beles Basin in Ethiopia. M.Sc Thesis, Royal Institute of Technology (KTH), Sweden.

Tadele, K. (2007). Impact of Land Use/Cover Change On Stream Flow: The Case of Hare River. Arbaminch University. Ph.D. Dissertation. Research institute for water and environment and Environment. Siegen University.

Tan, M.L., Ibrahim, A.L., Yusop, Z., Duan, Z., and Ling, L., (2015). Impact of Land Use and Climate Variability On Hydrological Components in The Johor River Basin, Malaysia. Hydrological Science Journal, Vol. 60(5): Pp873-882.

Teferi, E., Uhlenbrook, S., Bewket, W., Wenninger, J., and Simane, B. (2010). The Use of Remote Sensing to Quantify Wetland Loss in The Choke Mountain Range, Upper Blue Nile Basin, Ethiopia. Hydrol. Earth Syst.Sci., Vol(14): Pp.2415-2428.

Tekle, A. (2010). Assessment of Climate Change Impact On Water Availability of Bilate Watershed, Ethiopian Rift Valley Basin. M.Sc Thesis, Arba Minch University, Ethiopia.

Tekle, K. And Hedlund, L. (2000). Land Cover Changes Between 1958 And 1986 In Kalu District, Southern Wello, Ethiopia. Mountain Research and Development. Journal of Mountain research and development, Vol.20(1): Pp.42-51.

Tekleab, W (2015). Understanding Catchment Processes and Hydrologic Modelling in The Abbay/Upperblue Nile Basin, Ethiopia. Dissertation, Submitted in fulfillment of the requirements of the Board for Doctorates of the Delft University of Technology and the Academic Board of the UNESCO-IHE Institute for Water Education for the Degree of DOCTOR. Netherland, Pp.59-69.

Tesfa, G. And Bogale, G. (2016). Evaluation of Land Use Land Cover Change On Stream Flow: A Case Study of Dedissa Sub Basin, Abay Basin, South-Western Ethiopia, Author Profiles for This Publication. International journal of innovations in Engineering Research and Technology, Vol.3(8): Pp.44-59.

Teshome Y.B. (2016). Land Use Dynamics and Challenges of Enset (Ensete Ventricosum) Agriculture in The Upper Reaches of Baso-Deme Watershed, Gamo Highland, SW Ethiopia, Arba Minch University, Ethiopia.

Tolera K. (2018). Assessment of Land Use/Land Cover Change Impact On Stream Flow Using SWAT Model (The Case Study of Katar Catchment), A Thesis Submitted to The School of Graduate Studies of Addis Ababa University.

Tripathi, M. P., Panda, R. K. and Raghuwanshi, N. S. (2003). Identification and Prioritization of Critical sub-watersheds for Soil Conservation Management Using SWAT Model. BioSystems Engineering, Vol(85).

Tu, J. (2009). Combined Impact of Climate and Land Use Changes On Stream Flow and Water Quality in Easter Massachusetts, USA. J HYDROL, Vol(379): Pp.268-283.

Turner, W., Spector, S., Gardiner, N., Fladeland, M., Sterlin, E., and Steininger, M. (2003). Remote Sensing for Biodiversity Science and Conservation. Trends in Ecology and Evolution, Vol. 18(6): Pp. 306–314.

U.S. Army Corps of Engineers. (2001). HEC-HMS Hydrologic Modeling System User 'S Manual, Hydrologic Engineering Center, Davis, CA.

Van der Ent, R.J., Savenije H.H.G., Schaefli, B., Steele-Dunne, S.C. (2010). Origin and fate of atmospheric moisture over continents, Watwre resource research, vol(46), W09525,doi:10.1029/2010WR009127.

Wakjira, T., Tamene, A. and Dawud, T. (2016). The Effects of Land Use Land Cover Change On Hydrological Process of Gilgel Gibe, Omo Gibe Basin, Ethiopia. International Journal of Scientific & Engineering Research, Vol. 7(8): Pp. 118-128.

Ward, P.J., Renssen, H., Aerts, J.C.J.H., Van Balen, R.T. and Vandenberghe J. (2008). Strong Increases in Flood Frequency and Discharge of the River Meuse Over the Late Holocene: Impacts of Long-Term Anthropogenic Land Use Change and Climate Variability.

Webister, G. (2010). Hydrologic Impact of Land Use Change in The Upper Gilgel Abay River Basin, Ethiopia: Topmodel Application, MSc. Thesis, International Institute for Geo-Information Science and Earth Observation ENSCHEDE, The Netherlands.

Weng, Q.H. (2004). A Remote Sensing and GIS Evaluation of Urban Expansion and Its Impact On Surface Temperature in The Zhujiang Delta, China. International Journal of Remote Sensing, Vol. 22(10): Pp. 1999-2014.

Wogayehu B (2003). Economics of soil and water conservation: the theory and empirical application to subsistence farming in eastern Ethiopia highlands. Doctoral thesis, Swedish university of agricultural sciences, Uppsala.

Xia, Y.L., Fabian, P., Stohl, A. and Winterhalter, M. (1999). Forest Climatology: Estimation of Missing Values for Bavaria, Germany. Agricultural and Forest Meteorology, Vol. 96(1–3): Pp 131–144.

Yang, Z., Zhou, Y., Wenningers, J., and Uhlenbrook, S. (2012). The cause of flow regimes shifts in the semi-arid Humiliate river Northwest China. Hydrology and Earth system science, Vol(16): Pp 87-103.

Yenealem., M.B. (2018). Impact of LULCC On River Flow in The Lake Tana Basin, North Western Ethiopia. Dissertation Submitted to The Center for Environmental Science, Addis Ababa University, Ethiopia.

Yericho B.M. And Mulugeta, B.A. (2019). Challenges and Opportunities for Implementation of Integrated Water Resource Management in Omo Gibe Basin Ethiopia. Journal of Ecology and The Natural Environment, Vol.11(7): Pp. 84-97.

Yitae S.G. And Van Lanen, H. (2015). Assessing The Impacts of Land Use-Cover Change On Hydrology of Melka Kuntrie Subbasin in Ethiopia, Using A Conceptual Hydrological Model. Department of Natural Resources Management, Debre Berhan University, Ethiopia. Journal of Hydrology current research, Vol.6(3).

7. APPENDIXES

Appendix-1. Satellite Data for 1999, 2010, and 2018.

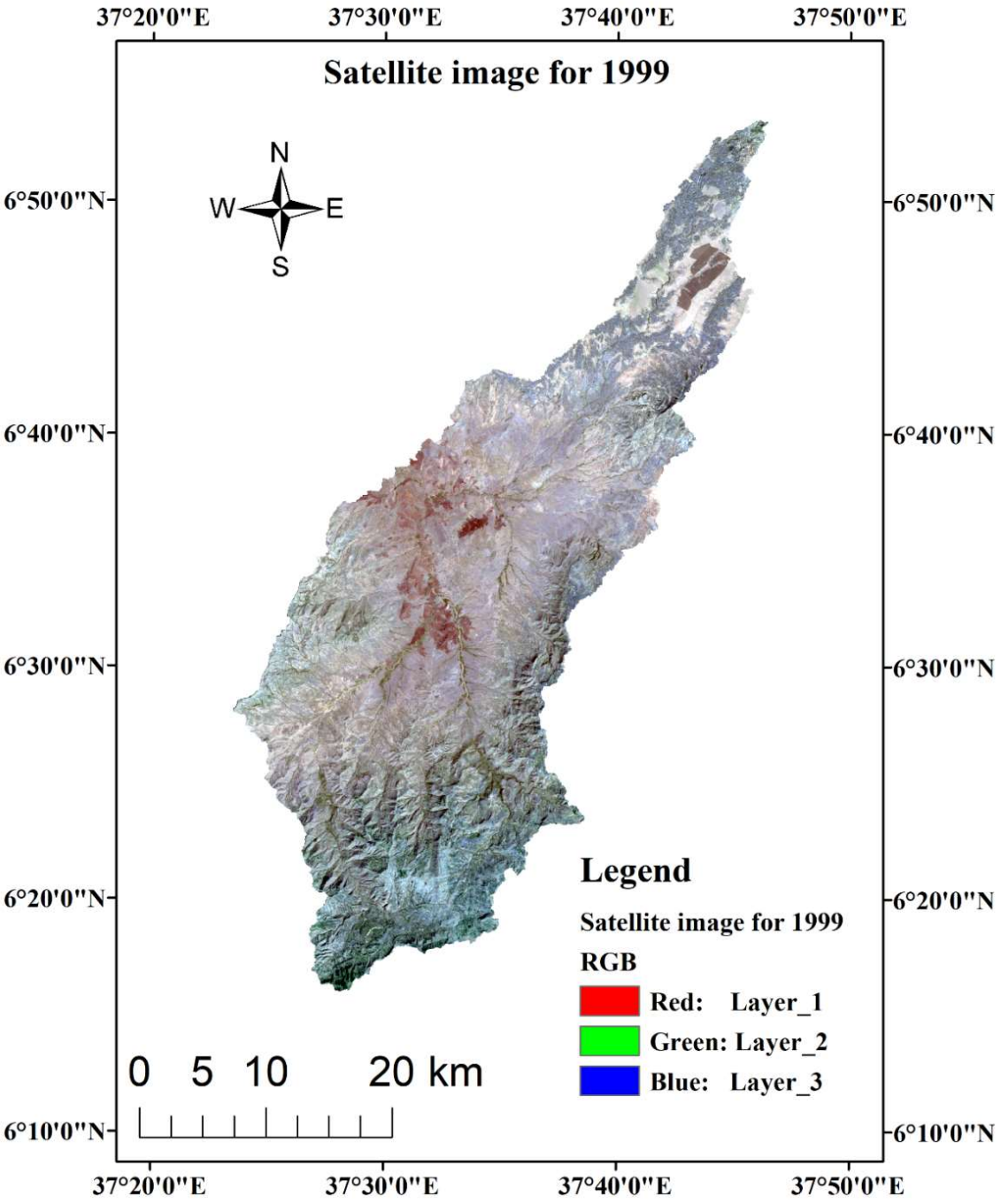

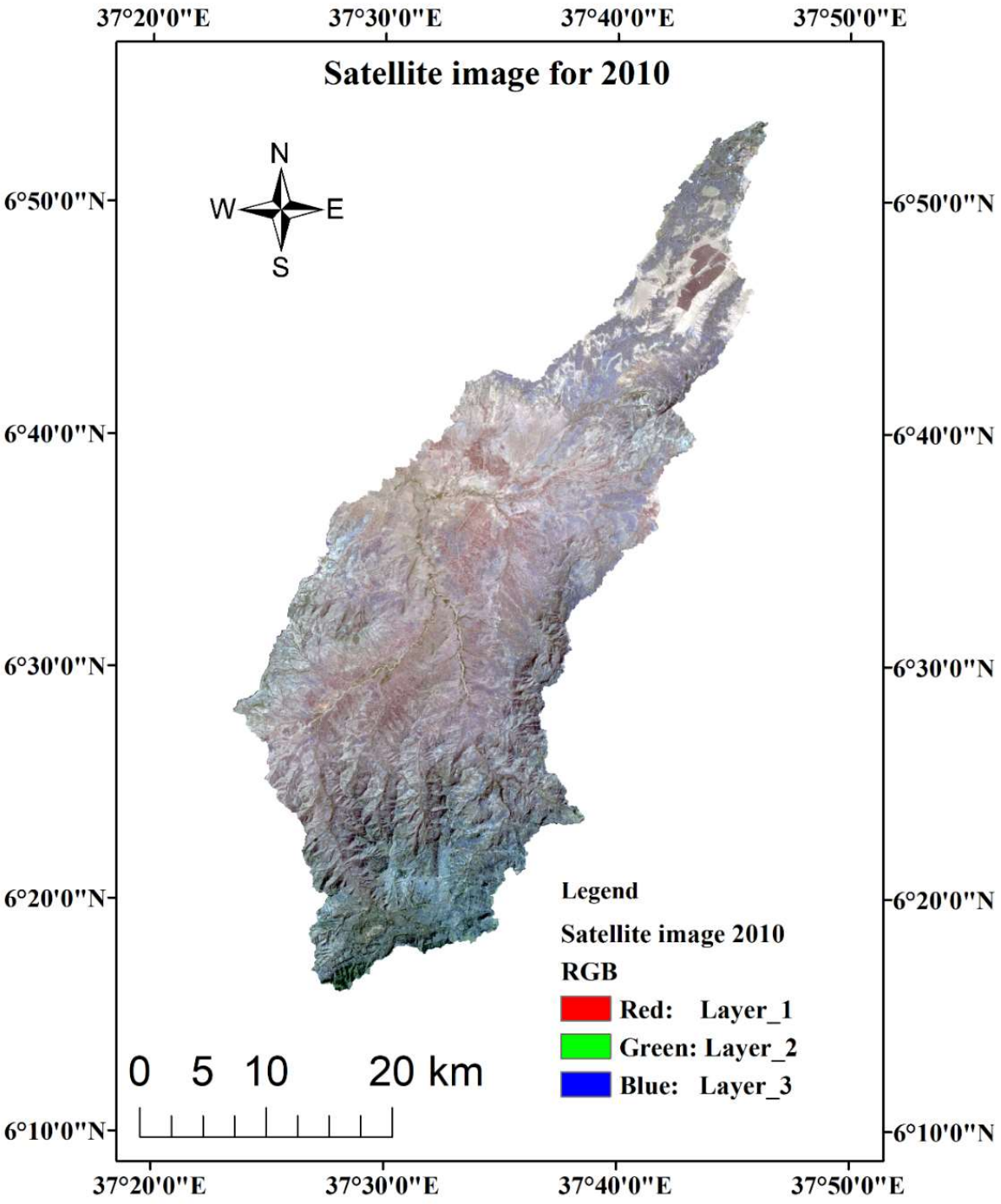
Satellite image for 2010
37°20'0"E
37°30'0"E
37°40'0"E
37°50'0"E
6°50'0"N
6°40'0"N
6°30'0"N
6°20'0"N
6°10'0"N
N
W
E
S
Legend
Satellite image 2010
RGB
Red: Layer_1
Green: Layer_2
Blue: Layer_3
0 5 10 20 km

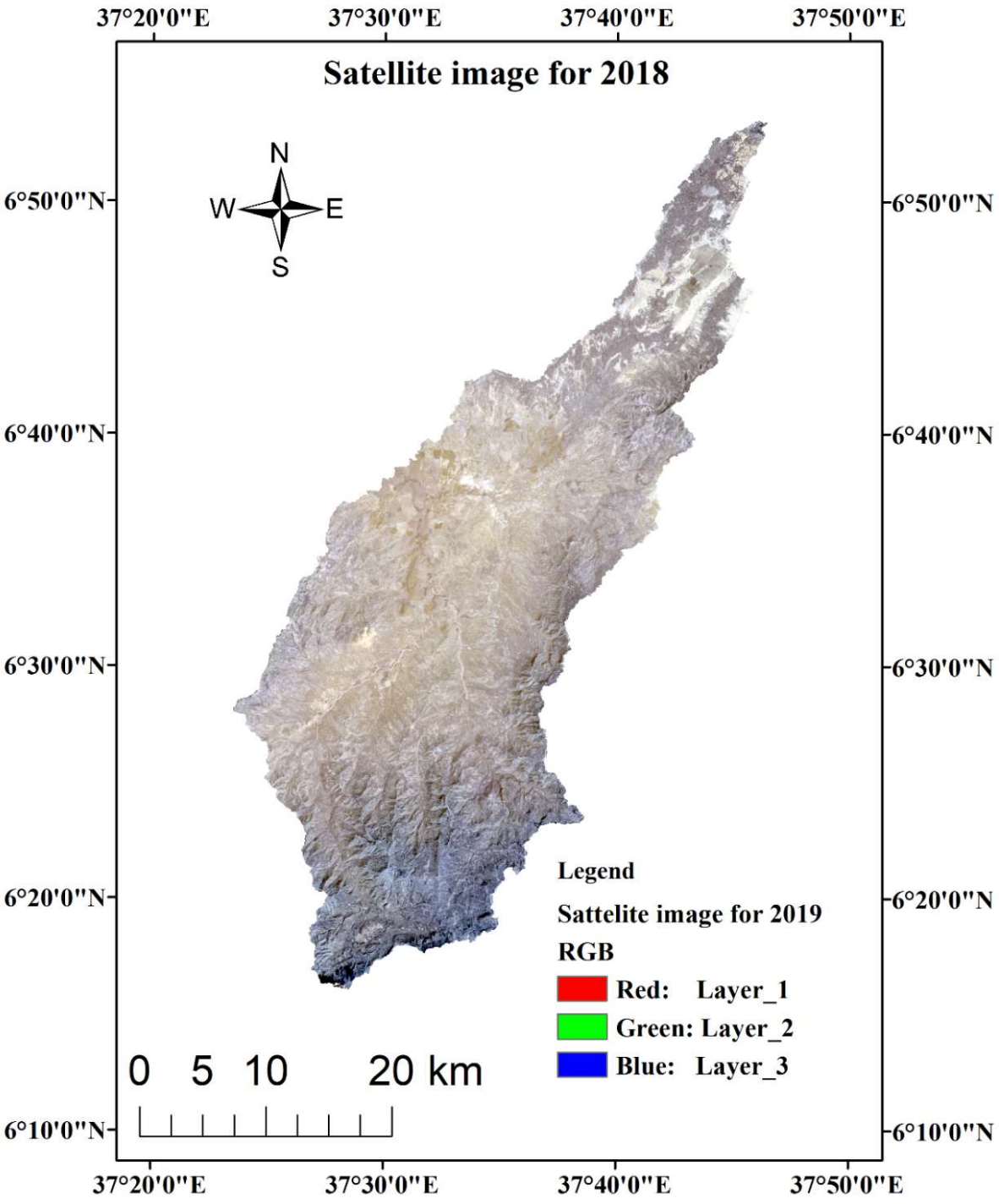
Satellite image for 2018
37°20'0"E
37°30'0"E
37°40'0"E
37°50'0"E
6°50'0"N
6°40'0"N
6°30'0"N
6°20'0"N
6°10'0"N
N
W
E
S
Legend
Sattelite image for 2019
RGB
Red: Layer_1
Green: Layer_2
Blue: Layer_3
0 5 10 20 km

Appendix-2. Mean annual Rainfall data for each station

Year	Gesuba	Danna 2	Dinke	sodo zuria
1989	1293.29	1427.46	1215.56	1567.16
1990	1159.07	1142.57	1119.77	1054.50
1991	1075.03	1062.99	1059.29	1209.74
1992	1255.36	1062.38	1415.78	1079.60
1993	1303.47	1349.87	1343.37	1788.25
1994	1443.18	1235.83	955.97	1639.98
1995	1186.85	935.60	1192.40	1300.08
1996	1362.98	1725.58	1218.19	1220.50
1997	1351.81	1315.29	1463.66	1423.41
1998	1287.75	1645.08	1411.57	1065.12
1999	1160.22	1167.83	1035.76	1480.40
2000	1447.33	1167.83	1042.92	1684.90
2001	802.28	1382.70	1319.84	1436.20
2002	698.23	1103.35	1354.47	1619.79
2003	1188.70	1086.98	1269.74	1326.40
2004	917.73	1004.64	1268.26	1283.00
2005	880.58	1745.75	1331.07	1045.70
2006	1378.01	1860.29	1275.70	1583.42
2007	1142.52	1840.31	1317.55	1362.20
2008	1216.92	1687.95	1287.11	938.20
2009	1031.05	1018.73	1386.13	1343.89
2010	1033.96	2060.02	1228.71	1458.30
2011	1665.30	1238.20	1164.35	1551.32
2012	1010.49	1134.30	1040.13	1080.20
2013	1486.62	1612.28	1196.01	1204.25
2014	1384.60	1741.17	1565.21	1443.50
2015	808.25	1375.98	838.95	1316.90
2016	962.14	780.79	1379.02	1112.70
2017	1417.36	1344.01	1184.93	1072.20
2018	1567.91	1751.72	1602.37	1275.90

Appendix-3. Wind speed, Temperature, Solar-Radiation of the station used for the study

year	Wolaita Wind	WOLAITA Temp. max.	WOLAITA Temp. min.	Wolaita solar	Geuba Temp. max	Gesuba Temp. max.
1989	1.85	24.70	13.36	6.68	14.52	28.00
1990	1.96	24.77	14.03	6.57	14.13	29.44
1991	1.80	25.04	14.44	6.68	15.40	28.43
1992	1.80	24.90	14.41	6.77	14.70	29.05
1993	1.86	25.18	15.08	6.82	14.78	29.09
1994	1.96	25.54	14.38	6.96	14.82	28.69
1995	1.78	25.79	14.42	6.85	15.08	28.76
1996	1.78	25.11	14.02	6.75	14.68	28.85
1997	1.82	25.58	13.80	6.86	15.41	28.92
1998	1.66	24.82	14.44	5.74	15.24	28.79
1999	2.06	25.34	14.61	5.93	14.51	28.86
2000	2.07	25.34	14.69	7.06	14.14	29.49
2001	1.61	24.91	14.38	6.51	13.03	29.36
2002	1.63	25.70	14.63	6.55	13.47	30.21
2003	1.67	25.45	14.84	6.99	13.60	29.70
2004	1.70	25.58	14.53	7.09	14.35	29.93
2005	1.51	25.30	14.50	7.01	14.43	29.65
2006	1.39	25.21	13.91	6.95	14.46	30.09
2007	1.53	25.34	13.91	6.83	14.49	29.92
2008	1.94	25.72	14.16	6.62	14.64	29.75
2009	1.51	26.04	15.05	7.02	15.43	30.22
2010	1.31	25.06	15.09	6.04	15.21	29.66
2011	1.55	25.66	15.14	6.57	15.02	28.47
2012	1.54	25.90	15.18	6.67	15.04	30.09
2013	1.29	25.15	14.71	6.27	15.24	28.57
2014	1.27	25.36	15.03	6.58	15.03	29.54
2015	1.40	26.34	15.45	6.77	14.71	29.63
2016	1.49	25.78	15.51	6.21	13.92	29.23
2017	2.04	26.34	15.39	6.22	14.15	28.08
2018	1.20	25.22	14.89	5.81	14.64	29.76

Appendix-4. Latitude, Longitude and mean annual Climatic value for the stations ued.

No.	Station name	Lat.	Long.	Rainfall (mm)	Temp Max. ^{0}C	Temp Min. ^{0}C	Relative humidity (%)	Wind speed (m/sec	Sunshine hours (Hrs.)
1	Wolaita sodo	6.8^0	37.7^0	1332.26	25.41	14.6	63.86	1.66	6.6
2	Gesuba	6.7^0	37.6^0	1197.3	29.26	14.61	-	-	-
3	Danna 2	6.6^0	37.6^0	1366.92	-	-	-	-	-
4	Dinke	6.4^0	37.4^0	1249.46	-	-	-	-	-

Appendix-5. Results for Sensitivity analysis

Parameter identifiers	t-Stat	P-Value	Rank
5:R__GW_REVAP.gw	0.02	0.98	16
15:R__CANMX.hru	0.29	0.77	15
10:R__HRU_SLP.hru	0.32	0.75	14
9:R__SOL_AWC(..).sol	0.38	0.71	13
13:R__REVAPMN.gw	-0.67	0.50	12
11:R__SLSUBBSN.hru	-0.69	0.49	11
4:V__GWQMN.gw	0.84	0.40	10
8:R__CH_K2.rte	-0.90	0.37	9
2:V__ALPHA_BF.gw	0.94	0.35	8
14:R__OV_N.hru	1.13	0.26	7
7:R__CH_N2.rte	-1.20	0.23	6
16:R__RCHRG_DP.gw	-1.41	0.16	5
3:V__GW_DELAY.gw	-1.76	0.08	4
6:R__ESCO.hru	1.96	0.05	3
12:R__SOL_BD(..).sol	5.38	0.00	2
1:R__CN2.mgt	42.43	0.00	1

Appendix-6. Soil layers and parameters used in SWAT model

NLAYERS	Number of layers in the soil
HYDGRP	Soil hydrologic group (A,B,C.D)
SOL_ZMX	Maximum root depth of the soil profile
ANION_EXCL	Fraction of porosity from which an ions are exchanged
SOL_CRK	Crack volume potential of the soil
TEXTURE	Texture of the soil
SOIL_Z	Maximum depth from soil surface to bottom layer
SOL_BD	Moist bulk density
SOL-AWC	Available water capacity of soil surface to bottom of the layer
SOL_K	Saturated hydraulic conductivity
SOL_CBN	Organic carbon content
CLAY	Clay content
SILT	Silt content
SAND	Sand content
Rock	Rock fragment content
SOL_ALB	Moist soil albedo

Appendix-7. Soils parameter value used in SWAT model

SNAM	LITHICLEPTOSOL	CHROMICLUVISOL	HUMICNITOSOL	EUTRICVERTISOL	HUMICALISOL
S5ID	ET1064	ET1154	ET1210	ET1282	ET878
CMPPCT	100	100	100	100	100
NLAYERS	1	2	2	2	2
HYDGRP	C	B	D	D	B
SOL_ZMX	100	1000	1000	1000	1000
ANION_EXCL	0.5	0.5	0.5	0.5	0.5
SOL_CRK	0.5	0.5	0.5	0.5	0.5

TEXTURE	Clay-Loam	Silt-Clay-Loam	Clay	Clay	Clay-Loam
SOL_Z1	100	300	300	300	300
SOL_BD1	1.44	1.47	1.33	1.3	1.43
SOL_AWC1	0.13	0.12	0.12	0.12	0.13
SOL_K1	7.78	8.73	1.37	1.13	5.26
SOL_CBN1	5.81	3.77	1.1	1.47	1
CLAY1	28	27	49	54	32
SILT1	29	22	27	25	29
SAND1	43	51	24	21	39
ROCK1	0	1	1	1	3
SOL_ALB1	0.01	0.13	0.0587	0.09	0.0712
USLE_K1	0.49	0.18	0.2329	0.2	0.2655
SOL_EC1	0	0	0	0	0
SOL_Z2	0	1000	1000	1000	1000
SOL_BD2	0	1.45	1.29	1.28	1.41
SOL_AWC2	0	0.12	0.13	0.11	0.13
SOL_K2	0	3.94	1.99	0.91	4.4
SOL_CBN2	0	1.74	0.5	1.37	0.4
CLAY2	0	34	61	56	32
SILT2	0	21	21	24	29
SAND2	0	45	18	20	36
ROCK2	0	0	0	1	1
SOL_ALB2	0	0.3	0.1867	0.09	0.2655
USLE_K2	0	0.17	0.2329	0.2	0.2655

Appendix-8. Mean monthly flow of Deme catchment

Yr./Mon.	JAN	FEB	MAR	APR	MAY	JUN	JUL	AUG	SEP	OCT	NOV	DEC
1989	0.81	0.87	1.03	4.10	2.42	2.77	3.39	2.39	5.36	6.92	1.49	2.40
1990	0.96	1.87	2.17	2.00	1.55	1.17	2.86	5.73	3.53	1.55	0.47	0.27
1991	1.47	1.57	4.17	1.71	4.86	5.86	6.12	4.23	5.79	3.21	1.23	0.91
1992	0.06	0.19	0.15	3.45	3.5	5.72	6.89	7.62	9.43	8.35	3.97	2.8
1993	2.75	4.12	2.05	4.73	13.86	8.08	15.3	5.06	3.61	6.43	2.3	1.01
1994	0.89	0.67	2.26	5.2	10.68	9.12	16.6	28.23	12.1	3.84	6.75	2.05
1995	0.76	0.58	2.3	4.72	3.81	6.2	10.7	6.33	9.68	2.53	1.12	0.21
1996	0.23	0.05	4.31	7.56	6.4	17.36	9.2	17.83	17.2	4.72	3.53	3.48
1997	2.58	2.32	2.16	4.25	2.76	2.58	5.31	3.88	2.01	8.75	13.7	6.23
1998	4.35	3.56	2.56	7.76	8.63	10.32	9.68	9.15	3.02	8.34	4.87	2.21
1999	2.56	1.61	2.02	1.95	2.21	6.04	6.85	8.56	5.13	4.71	2.23	1.61
2000	1.5	1.2	1.13	1.81	4.09	7.45	6.78	10.32	5.23	4.53	2.63	1.25
2001	0.93	0.84	1.66	2.19	9.78	5.32	6.54	5.44	7.56	7.23	1.27	1.41
2002	0.64	0.78	4.37	3.28	5.24	6.06	6.89	3.85	7.34	2.91	1.81	1.4
2003	0.54	0.34	0.67	1.25	7.31	4.23	2.92	4.73	5.96	1.85	0.92	1.43
2004	1.43	0.61	1.74	5.44	9.45	5.72	12.8	5.94	4.07	5.39	3.96	2.43
2005	1.9	2.15	3.35	6.12	11.34	4.79	12.6	14.35	8.63	2.53	1.56	0.77
2006	0.57	0.63	0.88	1.93	2.13	3.36	9.23	3.86	9.36	1.83	1.03	0.63

Appendix-9. Mean monthly and annual value for hydrologic components

1999 simulation result

MON	RAIN (MM)	AVE MON SNOW FALL (MM)	THLY BASIN SURF Q (MM)	VALUES LAT Q (MM)	WATER YIELD (MM)	ET (MM)	SED YIELD (T/HA)	PET (MM)
1	47.45	0	5.38	1.93	33.87	18.05	2.88	43.81
2	28.55	0	2.29	1.8	21.9	16.85	0.95	41.41
3	100.7	0	11.35	3.44	34.51	29.76	3.64	42.55
4	136.84	0	20.76	5.76	59.03	30.76	2.82	37.84
5	164.98	0	25.71	9.08	95.73	35.03	3.12	40.23
6	152.88	0	26.62	7.98	106.84	25.25	2.92	29.36
7	190.48	0	36.37	10.8	135.4	18.43	4.54	22.22
8	176.29	0	30.82	11.11	146.9	17.03	3.58	23.18
9	114.56	0	16.66	8.85	128.64	21.26	2.3	33.26
10	115.79	0	14.93	7.6	114.19	23.58	3.87	36.27
11	49.43	0	8.86	4.92	87.05	18.45	2.36	39.7

12	28.18	0	2.42	2.52	56.43	15.4	0.68	40.93

AVE ANNUAL BASIN VALUES

PRECIP = 1306.4 MM

SNOW FALL = 0.00 MM

SNOW MELT = 0.00 MM

SUBLIMATION = 0.00 MM

SURFACE RUNOFF Q = 202.20 MM

LATERAL SOIL Q = 75.81 MM

TILE Q = 0.00 MM

GROUNDWATER (SHAL AQ) Q = 705.47 MM

GROUNDWATER (DEEP AQ) Q = 37.19 MM

REVAP (SHAL AQ => SOIL/PLANTS) = 8.62 MM

DEEP AQ RECHARGE = 37.71 MM

TOTAL AQ RECHARGE = 754.22 MM

TOTAL WATER YLD = 1020.68 MM

PERCOLATION OUT OF SOIL = 757.28 MM

ET = 270.0 MM

PET = 431.1MM

2010 Simulation result

MON	RAIN (MM)	AVE MON SNOW FALL (MM)	THLY BASIN SURF Q (MM)	VALUES LAT Q (MM)	WATER YIELD (MM)	ET (MM)	SED YIELD (T/HA)	PET (MM)
1	47.45	0	5.69	1.77	34.06	17.97	3.08	43.81
2	28.55	0	2.44	1.65	21.91	16.7	1.04	41.41
3	100.7	0	12.07	3.17	34.95	29.6	4.82	42.55
4	136.84	0	22.02	5.28	59.67	31.21	3.58	37.84
5	164.98	0	27.24	8.28	95.89	35.55	4.13	40.23
6	152.88	0	27.97	7.27	106.66	25.62	4.31	29.36
7	190.48	0	38.33	9.85	135.4	18.35	6.81	22.22
8	176.29	0	32.61	10.17	146.86	16.3	5.39	23.18
9	114.56	0	17.63	8.11	128.43	20.73	3.35	33.26
10	115.79	0	15.89	6.98	114.4	23.15	4.6	36.27

11	49.43	0	9.29	4.51	87.04	18.23	2.69	39.7
12	28.18	0	2.61	2.3	56.42	15.29	0.77	40.93

AVE ANNUAL BASIN VALUES

PRECIP = 1306.4 MM

SNOW FALL = 0.00 MM

SNOW MELT = 0.00 MM

SUBLIMATION = 0.00 MM

SURFACE RUNOFF Q = 213.83 MM

LATERAL SOIL Q = 69.34 MM

TILE Q = 0.00 MM

GROUNDWATER (SHAL AQ) Q = 701.70 MM

GROUNDWATER (DEEP AQ) Q = 36.99 MM

REVAP (SHAL AQ => SOIL/PLANTS) = 8.62 MM

DEEP AQ RECHARGE = 37.51 MM

TOTAL AQ RECHARGE = 750.24 MM

TOTAL WATER YLD = 1021.87 MM

PERCOLATION OUT OF SOIL = 753.30 MM

ET = 268.8 MM

PET = 431.1MM

2018 simulation result

AVE ANNUAL BASIN VALUES

PRECIP = 1306.4 MM
SNOW FALL = 0.00 MM
SNOW MELT = 0.00 MM
SUBLIMATION = 0.00 MM
SURFACE RUNOFF Q = 229.77 MM
LATERAL SOIL Q = 59.38 MM
TILE Q = 0.00 MM
GROUNDWATER (SHAL AQ) Q = 697.03 MM
GROUNDWATER (DEEP AQ) Q = 36.75 MM
REVAP (SHAL AQ => SOIL/PLANTS) = 8.62 MM
DEEP AQ RECHARGE = 37.27 MM
TOTAL AQ RECHARGE = 745.35 MM
TOTAL WATER YLD = 1022.93 MM

PERCOLATION OUT OF SOIL = 748.40 MM
ET = 267.8 MM
PET = 431.1MM

MON	RAIN (MM)	AVE MONTHLY SNOW FALL (MM)	BASIN SURF Q (MM)	VALUES LAT Q (MM)	WATER YIELD (MM)	ET (MM)	SED YIELD (T/HA)	PET (MM)
1	47.45	0	6.13	1.55	34.43	17.89	2.45	43.81
2	28.55	0	2.64	1.44	21.97	16.54	0.92	41.41
3	100.7	0	13.1	2.72	35.51	29.38	6.17	42.55
4	136.84	0	23.74	4.48	60.33	32.08	4.88	37.84
5	164.98	0	29.24	6.98	95.8	36.61	5.94	40.23
6	152.88	0	29.82	6.12	106.11	26.38	7.24	29.36
7	190.48	0	40.99	8.33	135.02	18.3	11.44	22.22
8	176.29	0	35.03	8.71	146.64	15.23	9.15	23.18
9	114.56	0	19.02	7.02	128.22	19.89	5.29	33.26
10	115.79	0	17.26	6.06	114.82	22.24	4.51	36.27
11	49.43	0	9.89	3.93	87.27	17.92	2.41	39.7
12	28.18	0	2.88	2.02	56.58	15.15	0.68	40.93

Appendix-10. Iteration History for Calibration and Validation

Summary_stat.tx for Calibration

Iter 18 - Summary_Stat.txt | **Iter16 - Summary_Stat.txt** | Iter 16 - Observed_rch.txt | Iter 16 - 95ppu plot | Absolute_SWAT_Values.txt

Iter16 - Summary_Stat.txt

This file has the statistics comparing observed data with the simulation band through p-factor and r-factor and the best simulation of the current iteration by using R2, NS, bR2, MSE, and SSQR.

```
Goal_type= R2    No_sims= 300    Best_sim_no= 146    Best_goal = 7.919779e-001

Variable      p-factor  r-factor   R2     NS     bR2     MSE     SSQR     PBIAS    KGE     RSR    VOL_FR  ---  Mean_sim(Mea
FLOW_OUT_1      0.39      8.97     0.79   0.73   0.7560  5.1e+000 1.2e+000  23.7    0.81    0.52    0.88        5.84(5.12)


---- Results for behavioral parameters ---
Behavioral threshold= 0.500000
Number of behavioral simulations = 293

Variable      p-factor  r-factor   R2     NS     bR2     MSE     SSQR     PBIAS    KGE     RSR    VOL_FR  ---  Mean_sim(Mea
FLOW_OUT_1      0.39      8.96     0.79   0.73   0.7560  5.1e+000 1.2e+000 -14.0    -0.01    0.52    0.00        5.84(5.12)
```

Summary_stat.tx for Validation

Iter1 - Summary_Stat.txt

Iter1 - Summary_Stat.txt

This file has the statistics comparing observed data with the simulation band through p-factor and r-factor and the best simulation of the current iteration by using R2, NS, bR2, MSE, and SSQR.

```
Goal_type= R2    No_sims= 300    Best_sim_no= 14    Best_goal = 7.489476e-001

Variable      p-factor  r-factor   R2     NS     bR2     MSE     SSQR     PBIAS    KGE     RSR    VOL_FR  ---  Mean_si
FLOW_OUT_1      0.30      0.37     0.75   0.67   0.6646  3.8e+000 1.2e+000  25.7    0.76    0.57    0.84        4.79(4.


---- Results for behavioral parameters ---
Behavioral threshold= 0.500000
Number of behavioral simulations = 300

Variable      p-factor  r-factor   R2     NS     bR2     MSE     SSQR     PBIAS    KGE     RSR    VOL_FR  ---  Mean_si
FLOW_OUT_1      0.30      0.37     0.75   0.67   0.6646  3.8e+000 1.2e+000 -19.2    -0.01    0.57    0.00        4.79(4.
```

95PPU for Calibration

Iter16 - 95ppu plot

The 95ppu of all variables. Also shown are observations and best simulation of the current iteration.

Record 1 of 2 | Search

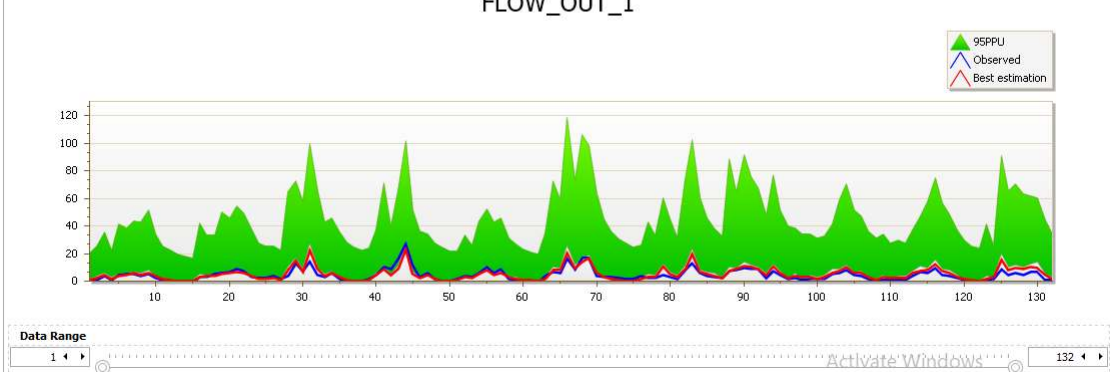

Data Range

1 | 132

Activate Windows

95PPU for Validation

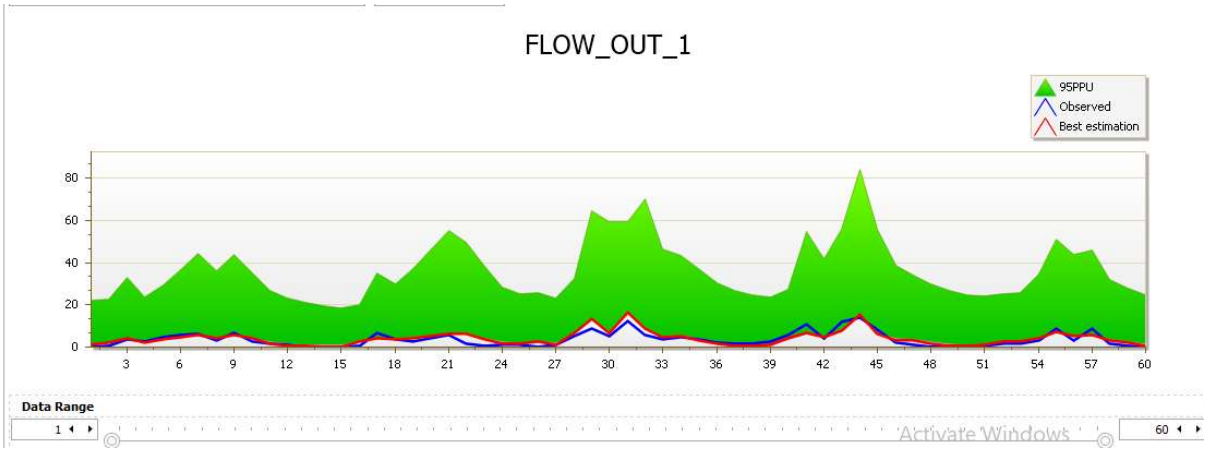

Appendix-11. Mean monthly simulated streamflow for LULC map of 1999, 2010, and 2010

Simulated Streamflow for 1999 LULC

	Jan	Feb	Mar	Apr	May	Jun	Jul	Aug	Sep	Oct	Nov	Dec
1991	2.80	4.78	1.80	3.31	3.93	5.28	3.79	5.19	4.35	1.93	1.21	1.56
1992	0.89	0.94	2.25	3.65	3.03	3.93	5.00	5.81	6.57	4.09	2.05	1.07
1993	3.25	1.96	7.03	14.80	6.09	16.34	7.79	4.13	5.87	3.73	1.74	2.34
1994	1.18	1.81	3.81	6.13	4.10	7.43	15.25	5.38	3.31	3.56	2.00	1.38
1995	1.25	1.86	2.48	2.21	3.81	7.00	4.52	5.15	3.29	2.33	1.20	1.38
1996	0.96	2.21	5.73	6.75	15.77	8.61	10.66	13.37	6.95	3.28	2.15	1.39
1997	1.39	1.08	0.90	2.28	2.65	8.20	4.28	3.24	7.81	15.39	7.76	1.75
1998	3.99	3.29	6.83	7.93	8.33	8.81	8.21	4.00	9.53	6.84	3.09	5.68
1999	3.81	3.75	1.65	1.57	3.52	6.52	7.73	5.63	6.12	3.51	1.75	3.15
2000	3.17	3.16	1.87	5.09	4.36	6.94	10.02	6.33	6.14	3.56	1.82	2.46
2001	1.30	2.39	2.73	12.73	6.97	7.65	8.25	6.41	8.40	5.28	2.46	1.47
2002	1.79	4.58	3.15	2.13	1.89	2.40	5.35	4.33	5.12	2.54	3.47	2.52
2003	2.12	1.60	1.06	1.67	4.23	6.93	10.62	6.43	4.40	2.24	3.20	4.00
2004	2.30	1.52	4.14	10.56	4.41	4.26	3.46	3.41	3.26	2.25	1.48	2.12
2005	2.86	4.83	6.06	14.78	6.18	9.03	7.22	9.04	7.74	6.24	2.91	2.08
2006	1.60	5.13	9.68	5.46	4.69	10.86	11.67	7.04	6.96	6.90	5.23	2.00

Simulated Streamflow for 2010 LULC

	Jan	Feb	Mar	Apr	May	jun	jul	aug	Sep	Oct	Nov	Dec
1991	2.28	4.07	2.26	3.99	4.70	5.05	6.24	4.77	4.18	1.90	1.19	1.22
1992	0.59	0.61	2.73	4.46	3.72	4.07	4.99	6.03	6.25	3.93	2.00	0.78
1993	2.73	1.59	7.28	14.64	7.01	7.36	17.04	9.25	5.62	3.60	1.72	1.94
1994	0.88	1.40	4.35	7.16	4.82	5.17	8.52	16.42	3.21	3.45	1.96	1.09
1995	0.93	1.45	2.95	2.80	4.59	4.94	8.00	5.60	3.17	2.26	1.19	1.09
1996	0.67	1.73	6.68	7.81	16.31	16.66	9.85	12.13	6.68	3.21	2.12	1.06
1997	1.10	0.79	1.16	2.83	3.33	3.68	9.45	5.34	7.92	15.07	7.38	1.46
1998	3.51	2.85	7.50	9.04	9.27	9.62	10.34	9.24	9.18	6.54	3.02	5.02
1999	3.28	3.19	2.04	2.03	4.08	4.43	7.98	9.12	5.85	3.39	1.72	2.78
2000	2.66	2.63	2.18	5.04	4.89	5.24	8.32	11.00	5.86	3.42	1.78	2.10
2001	0.99	1.95	3.32	13.11	7.91	8.26	8.87	9.25	8.09	5.06	2.40	1.18
2002	1.47	3.88	3.75	2.65	2.42	2.77	3.33	6.50	4.89	2.47	3.32	2.14
2003	1.77	1.26	1.44	2.24	4.97	5.32	8.23	11.48	4.23	2.18	3.10	3.43
2004	1.89	1.18	4.39	11.43	5.14	5.49	5.22	4.36	3.14	2.16	1.43	1.75
2005	2.35	4.47	6.54	15.61	7.06	7.41	10.10	8.54	7.41	6.04	2.84	1.66
2006	1.30	4.50	10.90	6.27	5.28	5.63	12.36	12.95	6.69	6.62	5.11	1.70

Simulated streamflow for 2018 LULC

	Jan	Feb	Mar	Apr	May	Jun	Jul	Aug	Sep	Oct	Nov	Dec
1991	1.90	1.90	3.58	5.39	6.18	7.87	6.48	8.10	3.74	1.68	1.00	0.58
1992	0.60	0.60	4.05	5.94	5.14	6.71	7.73	8.85	5.54	3.54	1.77	0.06
1993	1.67	1.67	8.30	15.22	8.62	18.80	11.23	6.70	5.03	3.23	1.52	1.40
1994	0.18	0.18	5.62	8.78	6.29	10.16	18.29	8.21	2.92	3.08	1.72	0.37
1995	0.25	0.25	4.20	4.18	6.07	9.58	7.37	8.02	2.84	1.98	0.99	0.38
1996	0.67	0.67	8.28	9.42	17.69	11.65	14.17	16.66	6.13	2.98	1.93	0.40
1997	0.39	0.39	2.32	4.16	4.77	11.43	7.09	5.80	7.82	14.42	6.63	0.75
1998	2.42	2.42	9.09	10.67	10.93	12.33	10.95	6.52	8.43	5.90	2.76	4.90
1999	2.93	2.93	3.31	3.33	5.47	9.92	11.09	8.55	5.23	3.06	1.53	2.21
2000	2.28	2.28	3.36	5.82	6.25	10.20	12.60	9.13	5.26	3.08	1.58	1.51
2001	0.31	0.31	4.70	14.28	9.49	10.65	10.85	9.29	7.46	4.57	2.17	0.48
2002	0.81	0.81	5.13	3.99	3.77	5.00	8.32	7.11	4.33	2.19	2.88	1.58
2003	1.16	1.16	2.69	3.59	6.38	10.12	12.85	9.52	3.82	1.95	2.75	3.17
2004	1.37	1.37	5.44	12.96	6.60	6.86	6.02	6.01	2.80	1.88	1.20	1.16
2005	1.97	1.97	7.99	16.87	8.64	11.77	10.45	12.17	6.72	5.54	2.59	1.14
2006	0.60	0.60	12.61	7.79	6.73	14.50	14.72	10.09	6.09	5.98	4.71	1.01